4-4-2016

Energy Transfer from Wind to Wave Groups: Theory and Experiment

Andrei Ludu
Embry-Riddle Aeronautical University, ludua@erau.edu

Shahrdad G. Sajjadi
Trinity College, Embry-Riddle Aeronautical Univeristy

Scholarly Commons Citation

Ludu, A., & Sajjadi, S. G. (2016). Energy Transfer from Wind to Wave Groups: Theory and Experiment. *Advances and Applications in Fluid Mechanics, 20*(1). https://doi.org/10.17654/FM020010021

Advances and Applications in Fluid Mechanics
© 2017 Pushpa Publishing House, Allahabad, India
http://www.pphmj.com
http://dx.doi.org/10.17654/FM020010021
Volume 20, Number 1, 2017, Pages 21-74 **ISSN: 0973-4686**

ENERGY TRANSFER FROM WIND TO WAVE GROUPS: THEORY AND EXPERIMENT

Shahrdad G. Sajjadi[1,2] **and Andrei Ludu**[1]

[1]Nonlinear Wave Laboratory
Department of Mathematics
ERAU
Florida, U. S. A.

[2]Trinity College
University of Cambridge
U. K.

Abstract

Three major unresolved problems that remain in oceanography are studied in depth, namely (a) unsteady waves, where waves are allowed to grow or decay in time and space; (b) sharp-crested waves (also known as fully nonlinear Stoke waves), which are note characteristic in oceans; and (c) group of waves, which can often become sharp-crested as they propagate downstream, as demonstrated here experimentally in a wave tank. The ultimate aim of such investigation is to improve the parameterization of the energy input from wind to waves. In this paper, we (i) present results on the simplest approximation to wave groups which result to a fully nonlinear Stokes waves (those having a sharp-crest); (ii) impose the boundary condition at the surface wave, rather than at the mean surface; (iii) assume the wave phase velocity is complex which consequently allows the wave amplitude to vary according to $a(t) = a_0 e^{kc_i t}$, where a_0 is the initial

Received: April 4, 2016; Accepted: December 18, 2016
2010 Mathematics Subject Classification: 74J15, 74J30, 76B15, 76-05.
Keywords and phrases: nonlinear waves, air-sea interactions, sharp-crested Stokes waves, wave tank experiment, wave groups.

constant amplitude, k is the wave number, and c_i is the wave complex phase speed; and, (iv) include the dominant viscous term in the perturbation equations. It is shown that: (i) yields an energy-transfer coefficient that is larger than that previously calculated for monochromatic waves and agree well with experimental data; (ii) has no major effect on the end-results; (iii) shows the variation of dimensionless energy-transfer parameter β with the wave age for unsteady waves; (iv) the vertical component of perturbation velocity is not singular at the critical point.

1. Introduction

This paper is concerned with the energy transfer from wind to a group of unsteady waves. However, before stating and outlining the problem which we shall pose and solve, we feel it is important to begin the introduction with an important review of major research and contribution made to the problem of wave generation by wind. After this historical review, we describe the motivation and need for the research undertaken, which we shall present in this paper.

1.1. A review of wave generation by wind and unresolved issues

In 1957, two independent theories of wave generation emerged on the strength of a review article by Ursell [59] (with its famous opening remarks: “Wind blowing over a water surface generates waves in the water by physical processes which cannot be regarded as known”). The analysis of Phillips [36] predicts that turbulent pressure fluctuations in the air generate small surface waves that grow linearly with time. In contrast, the contribution by Miles [29] leads to an exponential growth rate for waves.

Since then much research has been devoted to formulate a more physical and hence more realistic mechanism for wind-wave interaction which could be incorporated into spectral wave models. These spectral models solve the following equation for wind-wave evolution (Janssen [15-17]):

$$\frac{\partial \mathsf{F}}{\partial t} = \zeta \mathsf{F}, \tag{1.1}$$

where

$$\frac{\zeta}{\omega} = \sigma\beta\left(\frac{U_*}{c_r}\right)^2. \tag{1.2}$$

Here, $F(\omega)$ is the wave spectrum, ω is the angular frequency, ζ is the growth rate, σ is the ratio of air density ρ_a to water density ρ_w with a typical value of 1.275×10^{-3}, β is the non-dimensional energy transfer parameter, c_r is the real part of the wave speed[†], and U_* is the friction velocity. Many of these formulations solve ζ/ω directly, while others compute β then solve equation (1.2).[‡] The majority of previous research for the energy transfer parameter, β, is assumed to be a function of wave age c_r/U_*, roughness length y_0, and wave steepness *ak* (often taken to be $\ll 1$), where *a* is the wave amplitude (usually taken to be constant) and *k* the corresponding wave number. The wave steepness, being often taken to be very small, is commonly used in deriving expressions for β. Moreover, it often assumed that the wind and waves propagate unidirectionally, but this is not too severe a restriction since the effect of oblique wave propagation can easily be included by simply replacing U_* with $U_* \cos\theta$, where θ is the angle between wind direction and wave direction, in the final expression for β. The effect of large θ values and opposing wind/wave directions on equation (1.2) has been discussed in detail by Burgers and Makin [4] and Tolman and Chalikov [51].

Formulations for equation (1.2) have essentially emerged from three sources: analytical expressions; empirical fits to limited observation studies; and empirical fits to turbulent boundary layer models. Early analytical derivations for equation (1.2) were primarily confined to the work of Stewart [49], who conceived an expression for ζ/ω by combining theory with basic

[†]In spectral wave modes, *c* is assumed to be real and hence waves cannot grow and this is contrary to observation made in the sea.

[‡]The literature contains vastly confusing terminology for the energy transfer parameter, including often substituting ζ/ω with β and other variations. In this paper, we adopt the notation of Janssen [17].

experimental data of turbulent flow over rough surface, and most notably, Miles [29]. In Miles' quasi-inviscid theory, the criterion for the transfer of energy from a parallel shear flow to a traveling wave disturbance states that: "if a velocity profile has an inviscid neutral disturbance with non-vanishing wave number and phase velocity (equal to the velocity of the mean flow at some point in the profile), the disturbance with the same wave number is unstable when the Reynolds number is sufficiently large." The mechanism for this energy transfer is a Reynolds stress produced by a shift in phase between the two components of the perturbation velocity. In a nearly inviscid (high Reynolds number) flow such a phase shift may occur in the inner viscous layer, where the mean velocity relative to an observer moving with the wave reverses, or in the outer viscous layer in the neighbourhood of the wave surface.

Furthermore, Miles' [29] theory assumes the role of the Reynolds stresses is confined to the determination of the unperturbed mean velocity profile. For air owing concurrently with the waves, there is a height, the critical height, where the unperturbed wind speed equals the wave phase speed. (In the present study, where the effects of the turbulent stresses on the mean motion are considered, following Phillips [37] we use the term matched height.) The upward motion of the airflow over the wave induces a sinusoidal pressure variation which leads to a vortex sheet of periodically varying strength forming at the critical height. Then the vortex force (Lighthill [23]) on the wave leads to a transfer of energy from the wind to the waves. Note that according to this mechanism, the amplitude grows only if the wave is moving, i.e., for a fixed undulation (where the critical layer is at the wave surface) there is no asymmetric pressure and hence no wave growth.

Under these assumptions, the problem posed by Miles' model is a typical stability problem and is governed by the Rayleigh equation. By assuming the mean velocity profile is logarithmic, Miles analytically obtained an approximate solution to Rayleigh equation which he used to obtain an analytical expression for the energy transfer parameter β. This expression is a benchmark for other formulations of equation (1.2).

An alternative technique is due to Janssen [17] who solved the Rayleigh equation numerically. Surprisingly, his results solution differed with that of Miles'. Therefore, Janssen [17] derived his own expression for β through an empirical fit to his numerical solution, which has subsequently been used in spectral wave models such as WAM (Makin et al. [27]). Komen et al. [21] provide a similar derivation of the Rayleigh equation which includes the effect of atmospheric stratification based on the work of Janssen [17] and Janssen et al. [18] for more analysis of the numerical solutions to Miles' model.

A major inadequacy in Miles' theory is the neglect of any interaction between the waves and small-scale air turbulence, although turbulence is included in the model implicitly by prescribing a logarithmic velocity profile for the wind. Other contributions to wave growth not accounted for in Miles' theory include: the effect of wind gusts and large-scale turbulence (Komen et al. [21]), nonlinear interactions (Croft and Sajjadi [9]), interactions with sharp-crest waves (Croft and Sajjadi [9]), and the impact of additional vertical momentum fluxes where extremely fast wind regimes ($c_r/U_* < 5$, i.e., tropical cyclone conditions) result in saturated β values (Sajjadi [43]).

Turbulent interaction will alter the wind profile as well as its feedback to the waves thereby intensifying the growth rate for "slow moving" waves (young sea with small values of c_r/U_*), and increased damping of waves in the "fast moving" sea (swell regime with large values of c_r/U_*). However, the wave growth rates measured from field experiments show much larger values than that predicted by the Miles' mechanism (Dobson [10], Snyder et al. [48], Hasselmann [12]). Theoretical studies show the lack of turbulent interaction is one contributor to the underestimation (Sajjadi [41]) and Miles himself addresses this issue in subsequent studies (Miles [31-33], Ierley and Miles [13]). Jacobs [14] and van Duin and Janssen [60] construct analytical solutions to equation (1.2) through matched asymptotic expansions to eddy viscosity models which are surprisingly similar to the solution of Stewart [49]. However, Belcher and Hunt [1], based on rapid distortion theory, conclude that these growth rates in the young wave regime derived from

mixing length modeling were too large. Belcher and Hunt argue that the mixing lengths are being overestimated, since turbulence away from the water surface is slow with respect to the waves, and therefore large eddies do not have sufficient time to transport momentum to the waves.

Recently, in an award winning work, Sajjadi et al. [44] (SHD therein) showed that the non-separated sheltering (ignored by all above cited papers, except that of Belcher and Hunt) plays a major role in the energy transfer. Only in inviscid flows Miles' mechanism yields finite growth rate, due to the critical layer where at the critical point $U(y) = c_r$. Around the critical layer cats-eye pattern is formed which contributes to energy transfer from wind to water waves. However, Miles considered only the limiting case where the complex part of wave celerity tends to zero and consequently the critical layer is confined well within the inner layer close to the surface, see below. But SHD showed in the presence of finite eddy viscosity the flow field no longer exhibits singularity at the critical point. We remark that, in the non-separating sheltering theory the action of the Reynolds stresses close to the surface, in the inner region, cause a thickening of the boundary layer on the leeside of wave and thence to mean flow separation when the slope is large enough. The thickness of the inner region is therefore asymmetric and so, largely inviscid, outer region flow is asymmetrically displaced about the wave, leading to an out-of-phase component to the pressure perturbation. This mechanism is related to Jeffreys' [20] sheltering hypothesis, where the wave amplitude is of the order of the wavelength, which was developed for separated flows over moving waves of large slope to account for their growth.

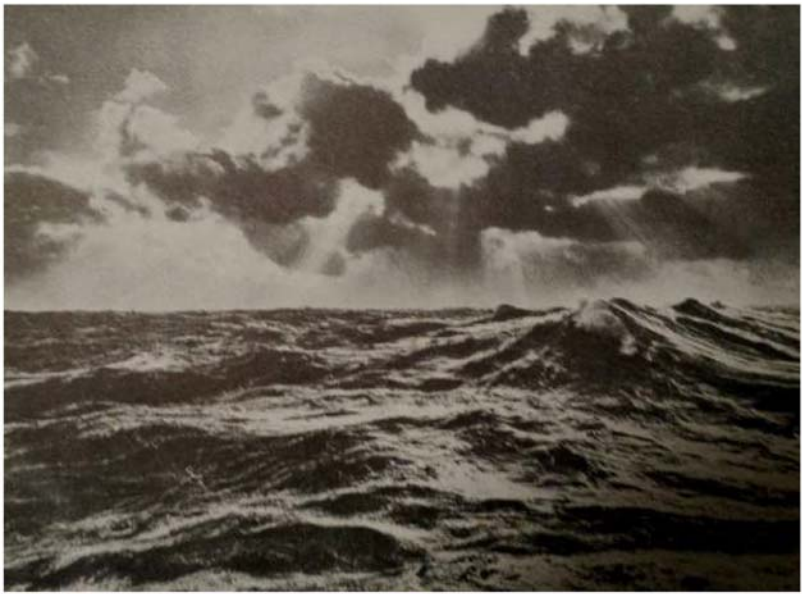

Figure 1. A photograph from the ocean showing group of waves forming a sharp-crested, or fully nonlinear Stokes waves.

Thus, the cats-eye formation is also due to the shear sheltering and diffusion in an inner viscous layer whose thickness ℓ is given by

$$k\ell \ln(\ell/y_c) = 2\kappa^2,$$

where y_c is the height of the critical layer, and κ in the von Kármán's constant. It is to be noted that in the inner layer as the surface is approached, the turbulence tends to a local equilibrium so that it adjusts to the local velocity gradient. The asymmetry of the mean flow, and hence the mean flow gradients, in the perturbed boundary layer therefore lead to asymmetrical perturbations in both the normal and shear Reynolds stresses. These asymmetrical perturbations to the Reynolds stresses at the surface also lead to an amplification of the wave (Townsend [55, 57]). Stewart [49] and Longuet-Higgins [25] have discussed this mechanism for the transfer of energy into the wave motion, but they did not study the effect as part of a systematic analysis.

SHD also showed that as wave steepness assumes the physical oceanographic situation where wave speed $c = c_r + ic_i$, the critical height rises and for very steep waves $ky_c > kl$. Furthermore, these steep waves exhibit a sharp-crest (see Figure 1), consequently they are referred to as fully nonlinear Stokes waves which are often result from interactions of several harmonic waves, namely group of waves.

To study energy transfer from wind to fully nonlinear Stokes waves, Sajjadi [41] combined an eddy viscosity formulation (Sajjadi et al. [40]) close to the wave surface with a rapid distortion formulation above the waves and derived an analytical expression for β from an inhomogenous Rayleigh equation for each harmonic of waves. His derivation, valid for $c/U_* > 5$, included perturbation equations for Reynolds stresses thereby the effect of turbulence was included explicitly in his model. Moreover, this equation contained two terms which quantified the individual contributions of the Miles' mechanism and the effect of turbulence. Most significantly, this equation matched the expected profile of β, showing growth of slow moving waves $(5 < c_r/U_* < 20)$, maximum growth in the intermediate region $(10 < c_r/U_* < 40)$, damping of fast moving waves $(20 < c_r/U_* < 40)$, and decay $(\beta < 0)$ for $c_r/U_* > 40$. However, since this expression had to be summed over all harmonics, is not very practical for incorporation into spectral wave models.

Wave growth formulations based on empirical fits to field studies have provided valuable insight into wave physics, but the accuracy of these algorithms is still questionable. Plant [38] showed β is approximately constant with a value of 30 for $0.3 < c_r/U_* < 12.5$, which is roughly double that obtained by Townsend [55]. From a field study conducted in the Bahamas, Snyder et al. [48] derived an empirical parameterization for wave growth which is a function of the 5 m wind speed (U_5) valid for $0.1 < c_r/U_5 < 0.3$. From scaling arguments, Komen et al. [21] suggested a modified wave growth parameterization with $U_5 \approx 28U_*$ (making the parameterization valid

roughly for $3 < c_r/U_* < 14$), and this Snyder-Komen formulation has been used in many studies as well as options in spectral wave models such as WAM (WAM [19]) and WAVEWATCH (Tolman and Chalikov [51], Tolman [52, 53]). The measurement of energy transfer from wind to waves is a difficult task, particularly since in most experiments sensors measure the wave-induced pressure fluctuations at a fixed height above the water surface as performed in most experiments (Burgers and Makin [4], Janssen [17]). In these situations, the measurements are extrapolated to the water surface, usually by assuming an exponential decay. However, this methodology is not very fruitful since the results are very sensitive to the decay parameters used. Furthermore, it is difficult to distinguish the effects of dissipation and wave-wave interaction from the wind-wave interactions. Applying regression models to a limited sample for an incomplete range of c_r/U_* also suffers from over-fitting and other statistical issues, as well as a tendency applying these equations outside the original range of their validity.

As an alternative to using wave data or analytical derivations, several researchers have derived empirical expressions from the numerical model results of turbulent boundary layer flow over a moving (usually monochromatic) gravity surface wave. A team of Russian scientists first used this approach, studying the effect of small-scale turbulence on wave growth using two-dimensional Reynolds stress equations (Mastenbroek et al. [28], Sajjadi and Drullion [47]). This work has culminated in the most complex formulations for equation (1.2) to date, with piece wise linear and quadratic empirical equations for different intervals of c_r/U_λ, where U_λ is the wind speed at the wave height (assumed to be equal to the wavelength). Also, wave growth is sensitive to the value of the drag coefficient C_D, but as an example, for $C_D = 2 \times 10^{-3}$, these formulations yield positive values of β in range $0.04 < c_r/U_\lambda \leq 0.8$ which are largest for young waves, but decrease approximately linearly in the intermediate range. However, in the range $0.8 < c_r/U_\lambda < 1.6$ as well as the range $-1.25 < c_r/U_\lambda < 0$, for which the wind blows against the waves, negative values of β are obtained. From the

relationship $U_* = \sqrt{C_D} U_\lambda$, these ranges which correspond to $0.8 < c_r/U_* < 17$, $17 < c_r/U_* < 34$, and $-26 < c_r/U_* < 0$, respectively. Note incidentally, the Burgers and Makin [4] formulation is the default expression for equation (1.2) in WAVEWATCH (Tolman and Chalikov [51], Tolman [53]).

Finally, because waves grow by extracting momentum from the air, the treatment of surface stress, which crucially depends on surface roughness y_0, is very important in wave growth formulations. In addition to turbulent Reynolds stress τ_{turb} based on mixing length theory, air flow over growing waves also lose momentum due to pressure differences upwind and downwind of the wave crest, the so-called "wave-induced" stress τ_{wave} (Janssen [16, 17]). The result is that the total stress $(\tau_{total} = \tau_{turb} + \tau_{wave})$, being generated by wind, is larger for young waves $(c_r/U_* < 15)$ than those for old waves in the swell regime $(c_r/U_* > 20)$. Several observational studies confirm that y_0 is a function of wind speed and wave age. For example, Donelan et al. [11] and Maat et al. [26] have shown that y_0 is inversely proportional to wave age. Indeed, several studies (Nordeng [35], Janssen [17], Makin et al. [27], Chalikov [5]) have adopted an expression for y_0 that have aforementioned wave age dependency. Note that, y_0's dependency on wind speed and wave age results in an implicit relationship that often requires iterative procedures to obtain equation (1.2); this is also impractical for use in spectral wave models. The sensitivity of wave growth to these different wave age based y_0 formulations has not yet been examined in much detail.

For oceanographic purposes, there are three major unresolved problems remaining to be studied in depth: (a) unsteady waves, where waves are allowed to grow or decay in time and space; (b) non-monochromatic waves, as such waves do not exist in the ocean; and (c) group of waves, which can often become sharp-crested as they propagate - they are characteristics of waves observed in the ocean. To date, none of the above points (a)-(c) has been investigated in depth. But the result of such investigation is required in

order to improve the parameterization of the energy input from wind to waves. In this paper, as in SHD, and Sajjadi and Drullion [47], we attempt to resolve some of these issues and offer alternative expressions for them.

1.2. The present contribution

Thus, the aim of this paper is to: (i) present results on the simplest approximation to wave groups which results to a fully nonlinear Stokes waves (namely sharp-crested waves); (ii) impose the boundary condition at the surface wave, rather than at the mean surface; (iii) assume the wave phase velocity is complex and consequently the wave amplitude is taken to be $a(t) = a_0 e^{kc_i t}$, where a_0 is the initial constant amplitude; (iv) include the dominant viscous term in the complete Orr-Sommerfeld equation; and (v) confirm the earlier conjecture by Croft and Sajjadi [9] that this increased energy transfer is due to the steepness of fully nonlinear Stokes waves and show how much of this increased energy is transferred to higher harmonics. We shall find that: (i) yields an energy-transfer coefficient that is larger than that previously calculated for monochromatic waves; (ii) has no real effect on the end-results; (iii) shows how β varies for an unsteady waves; (iv) shows that the viscous effects in the air just above the surface wave are small compared with those in the water, being of relative order $\sigma R_a^{-1/2} R_w$, where

$$R = c_r / k\nu \tag{1.3a}$$

or for gravity wave,

$$R = c_r^3 / g\nu \tag{1.3b}$$

denotes a Reynolds number based on wave speed, wave number, and the viscosity of either fluid (suffices *a* and *w* denote air and water, respectively); and (v) shows order of magnitude agreement with oceanographic observations. We will also show the damping ratio is given by

$$kc_i = \zeta = \frac{2\mathscr{I}\{\sqrt{\mathscr{F}_1 + k^2 a^2 \mathscr{F}_2}\}}{\mathscr{R}\{\sqrt{\mathscr{F}_1 + k^2 a^2 \mathscr{F}_2}\}},$$

where the expressions for $\mathscr{F}_i$, $i = 1, 2$ is given in Section 6, has additional

components proportional to k^2a^2 for wave groups compared with the corresponding expression for the monochromatic wave. This indicates that the extra energy is transferred to group of waves via the presence of $\mathscr{F}_2$ term whose magnitude is less than $\mathscr{F}_1$ but its overall effect is to increase the magnitude of ζ and hence yield an additional energy transfer from wind to group of waves.[†]

Although, we recognize that the turbulent stresses will profoundly affect the wave growth (Miles [31], Sajjadi [41]), however, in the present model, the role of the Reynolds stresses is confined to the determination of the unperturbed mean velocity profile. For air owing concurrently with the waves, there is a critical height where the unperturbed wind speed equals the wave phase speed. The upward motion of the airflow over the wave induces a pressure variation which leads to a vortex sheet of periodically varying strength forming at the critical height. Then the 'vortex force' on the wave leads to a transfer of energy from wind to the waves. We will show that the growth rate, for each harmonic of a nonlinear wave, consists of three components. The first is a positive energy-transfer from the shear flow, being essentially the same as the inviscid mechanism of Miles [29]. The second and the third components represent, respectively, additional energy transfer from viscous dissipation in the air and the water. We will further demonstrate that simple asymptotic expressions, used in the most large-scale wave models, lead to growth rate that is a factor of $O(1/\varepsilon)$, too large, where

$$\varepsilon \sim \frac{1 + c_r/U_*}{(1/\kappa)\ln(\lambda/y_0)}.$$

Here, we will offer an alternative expression which agrees better with both experimental and numerical data.

In this paper, we shall develop the equations of motion for the water in

[†]Note that for monochromatic waves ($\mathscr{F}_2 \equiv 0$) the expression for ζ reduces to that found by Miles [30].

Section 5 on the assumption $S_w \ll 1$, where [based on $\rho_a U_*^2 = \rho_w \nu_w U'(0-)$],

$$S_w = U'(0-)/kc = \sigma U_*^2 / kc\nu_w. \qquad (1.4a, b)$$

This permits the neglect of the shear flow in the water and the derivation of our results directly from Lamb [22, Section 349].

Having developed the equations of motion in Sections 4 and 5, we shall impose the boundary conditions of continuity of velocity and stress in Section 6 to obtain an approximation to the complex wave speed. We assume that the magnitude of the wave speed is closely approximated by its unperturbed, inviscid value [$c_r^2 = gk^{-1}(1 + k^2 a^2)$ for gravity waves] and that this value may be used in the determination of the perturbation flows. In the Appendix, we shall present numerical results, based on revised and extended analysis originally offered by Conte and Miles [8].

One of the major components of next-generation operational models includes coupling interaction between meteorology and wave models. However, software tools to facilitate coupling are currently unavailable, requiring major computer coding of both models to include interactions during time steps and also developing new computer architecture, such as code parallelization, to accelerate the solution schemes.

Most wave models to date are based on non-physical or ad-hoc parameterization of source terms, often empirically derived, which often yields to an inaccurate solution. For example, underestimation of wave growth due to wind-wave interaction is a well-known problem in current wave models, and attempts to address this problem are often crude. In recent years, Sajjadi et al. [40, 42], Sajjadi [41] and SHD have identified that the underestimation in wave models is due to the neglect of turbulent interaction between the atmosphere and ocean, and due to a lack of consideration for different phase speeds and nonlinearity in surface wave profiles. Nearly all parameterizations follow the original critical-layer contribution made by Miles [29] which only accounts for wave growth due to inviscid shear-flow instability, and assumes the wind speed is low compared to the wave speed.

In Section 7, we will compare the result of the present parameterization with those of Miles [29], Janssen [17] and experimental data.

2. The Effects of Grouping on Wave Growth

When there is a significant mean flow above the interface, inertial forces become comparable with the buoyancy forces and the Froude number $\mathcal{F}_I \sim 1$, where $\mathcal{F}_I = U_*^2/(\mathcal{G}\lambda)$, and $\mathcal{G} = 2(\rho_w - \rho_a)/(\rho_w + \rho_a)$. A number of mechanisms have been proposed for how such an airflow over a horizontal body of liquid produces waves on its surface (Sajjadi et al. [42]). Most of those proposed have been linear and therefore can be applied to any spectrum of waves. But the mechanisms and models based on them are regularly applied when the surface disturbances significantly affect the gas and liquid flows, so that the mechanisms are nonlinear, and the waves are not monochromatic. Typically the waves move in groups, which affect how the wind flows over the waves, how the waves break and thence how droplets form. This weakly nonlinear interaction of mechanisms significantly influence the average momentum, heat and mass transfer associated with waves. Very small unsteady waves are initiated by turbulence and/or growing Tollmien-Schlichting instabilities in the sheared airflow over the surface and Kelvin-Helmholtz coupled instability of the airflow over the liquid (Tsai et al. [58]). When steady waves are generated artificially in an airflow, e.g. in a wind-wave tank, the linear mechanisms for the growth of the waves are the pressure drag caused by asymmetric slowing of airflow over the downwind slopes of the waves and turbulence stresses caused by the disturbed flow, and wind-induced variations of surface roughness disturbed surface (Belcher and Hunt [1, 2]). Both mechanisms are affected by the relative speed of the wave, c_r, to the friction velocity, U_*, of the airflow, and the disturbed flow changes at the critical height.

Consider when the waves, with wavelength $2\pi/k$, begin to grow at a rate kc_i. If this is comparable with the frequency of wave passing, i.e. U_*k, then the critical layer is above the inner shear layer near the surface. Also, the

dynamics across the critical layer are determined by inertial forces as the flow accelerates and decelerates over the wave. But only if the wave is growing (or decaying), i.e., $c_i \neq 0$, is there a net force on the wave caused by critical layer dynamics (Belcher et al. [3]). Their triple deck analysis agrees with that of Miles' [29] different method of analysis for a growing wave. Hence they do not agree with him, and many subsequent authors' (e.g., Lighthill [23]), conclusion is that there is a net inviscid force on monochromatic non-growing waves (i.e. $c_i = 0$).

This conclusion of Miles' has been used to correlate data on the growth of wind-generated waves, and became the standard model for ocean forecasts, etc. (Janssen [19]). Subsequently this was contested by several authors, both on mathematical and physical grounds, (e.g. Mastenbroek et al. [28]). They showed that similar predictions for the magnitude of average wave growth correlations could be derived by the viscous/turbulence sheltering mechanism (Belcher and Hunt [1]). But this perturbation sheltering theory which assumes c_r is small, is found experimentally to be an under estimate for the force on waves when c_r is comparable with the mean wind speed. One interaction of wind with group of waves reason is that it does not represent the dynamics of waves which grow and decrease in groups.

A conceptual model has been developed for the laminar/turbulent shear flow over steadily moving wave groups. Weakly nonlinear theory is used to analyze the disturbed airflow over the waves in groups, which shows how the airflow over the downwind part of the group is lower than over the upwind part. This asymmetry causes the critical layer height y_c to be higher and the wind shear at y_c to be weaker over the downwind part. Therefore, the positive growth of the individual waves on the upwind part of the wave group exceeds the negative growth on the downwind part (which would not be true if y_c was the same over the whole group). This leads to the critical layer group (CLaG) effect producing a net horizontal force on the waves, in addition to the sheltering effect. This analysis is supported by numerical simulations (e.g. Touboul et al. [54]).

Wave shapes also affect the wave growth (e.g. Sajjadi et al. [42]). Whether (as in the photographs in Jeffreys [20]) the wave groups are capillary waves on a Cambridge duck pond or breaking rollers in the Atlantic ocean, the wave shapes as well as their height vary in a group. Since their slopes tend to increase downwind, this is likely to amplify the CLaG mechanism. By considering the dynamics of typical wave groups, it becomes possible to estimate rationally how airflow affects the nonlinear interactions between waves, and compare how this relates to the wave-wave hydrodynamic interactions, that are assumed to dominate the distribution of ocean waves. Thus variations of wave shapes within a group could also affect the net wave growth, while violent erratic winds can prevent the formation of wave groups, so that wave growth may be reduced (but spray from waves is increased) as is observed near the centre of hurricanes.

At higher wave speeds, another mechanism is also significant, namely the displacement of the critical layer outside the surface shear layer (i.e. $c_r > U_*$). This acts to reduce the sheltering mechanism, by contrast with Belcher and Hunt [1] analysis (when $c_r < U_*$) which showed how the critical layer within the shear layer increases the sheltering mechanism (see Cohen and Belcher [7]). Thus the decrease of the growth rate as c_r/U_* increases is compensated by the increase in growth rate as waves form into groups at higher wind speeds (which also needs to be modeled). The decrease in the local sheltering mechanism as y_c increases over the downwind part of a wave group further affects the dynamical effect of the critical layer. (We note that the existence of a critical layer over a monochromatic with a significant role on the boundary layer dynamics still does not mean that the Miles inviscid mechanism is operative (cf. Sullivan et al. [50]).)

3. Group of Waves on Deep Water

We have to consider the transmission of disturbances in a medium for which the velocity of propagation of homogeneous simple harmonic wave-trains is a definite function of the wavelength. The kinematically simplest group of waves is composed of only two simple trains, of wavelengths λ and

λ_1 differing by an infinitesimal amount $d\lambda$: then with the usual approximation we have for the combined effect

$$y = a\cos[k(x - ct)] + a\cos[k_1(x - c_1 t)]$$

$$= 2a\cos[\pi\lambda^{-2} d\lambda(x - c_g t)]\cos[k(x - ct)], \tag{3.1}$$

where

$$c_g = c - \lambda\frac{\partial c}{\partial \lambda} = c + k\frac{\partial c}{\partial k} \tag{3.2}$$

and $k = 2\pi/\lambda$ is the wave number.

The expression (3.1) may be regarded as representing at any instant a train of wavelength λ, whose amplitude varies slowly with x according to the first cosine factor. Thus it does not represent a form which moves forward unchanged; but it has a certain periodic quality, for the form at any given instant is repeated after equal intervals of time $\lambda/(c - c_g)$, being displaced forward through equal distances $\lambda c_g/(c - c_g)$. The ratio of these quantities, namely $\mathscr{C}$, is called the *group-velocity*. It has also the following significance: in the neighbourhood of an observer traveling with velocity c_g the disturbance continues to be approximately a train of simple harmonic waves of length λ.

The most general simple, or elementary, group may be defined in the following manner. Let the central from be a simple harmonic wave of length $2\pi/k_0$, and let the other members be similar waves whose amplitude, wavelength, and velocity differ but slightly from the central type; then, with similar approximation, we have

$$y = \Sigma a\cos\{k(x - ct) + \theta\}$$

$$= \Sigma a_n\cos\{k_0(x - c_0 t) + (x - c_{g0} t)\delta k_n + \theta\}. \tag{3.3}$$

The range of values of k being infinitesimal, the group as a whole may be written, as in the previous case, in the form

$$y = \phi(x - c_{g0}t)\cos\{k_0(x - c_0t) + \varpi\}, \tag{3.4}$$

where ϕ is a slowly varying function; and the group-velocity c_{g0} is given by

$$c_{g0} = \frac{d}{dk_0}(k_0c_0). \tag{3.5}$$

The group, to an observer traveling with velocity c_{g0} appears as consisting of approximately simple waves of length $2\pi/k_0$. The simple group is, in fact, propagated as an approximately homogeneous simple wave-train; the importance of the group-velocity lies in the fact that any slight departure from homogeneity on a simple wave-train, due to local variation of amplitude or phase, is propagated with the velocity c_g.

3.1. The Fourier integral regarded as a collection of groups

An arbitrary disturbance can, in general, be analyzed by Fourier's method into a collection of simple wave-trains ranging over all possible values of *k*; thus after a time *t* the disturbance will be given by an expression of the type

$$\int_0^\infty \phi(k)\cos[k(x - ct + \theta)]dk, \tag{3.6}$$

where *c* is a given function of *k*.

The method adopted with these integrals is based on Lord Kelvin's treatment of the case, in which the amplitude factor $\phi(k)$ is a constant, so that

$$\int_0^\infty \cos[k(x - ct + \theta)]dk.$$

An integral solution of this kind is constructed to represent the subsequent effect of an initial disturbance which is infinitely intense, and concentrated in a line through the origin; Lord Kelvin's process gives an approximate evaluation suitable for times and places such that $x - ct$ is large, and the argument may be stated in the following manner:

In the dispersive medium the wave-trains included in each differential element of the varying period are mutually destructive, except when they are in a same phase and so cumulative for the time under consideration, this being when the argument of the undulation is stationary in value. Thus each differential element as regards period, in the Fourier integral, represents a disturbance which is very slight except around a certain point which itself changes with time.

Applying the method to the more general integral (3.6), we obtain an expression for the total disturbance, attending only to its prominent features and neglecting the rest, provided we assume the change of the amplitude factor $\phi(k)$ to be graded. On this hypothesis the resulting expression contains the amplitude of the component trains simply as a factor; and in this way the trains for which it is a maximum show predominantly in the formal which exhibits the main features of the disturbance as they arise from place to place through cumulation of synchronous component trains.

The argument shows that in some respects the integral (3.6) may be more conveniently regarded as a collection of traveling groups instead of simple wave-trains; when $\phi(k)$ is a slowly varying function, the groups will be simple groups of the type (3.3). The limitations within which this is the case will appear from the subsequent analysis; one method of procedure would be graphical: to take a graph of the fluctuating factor and see that the other factor, which is taken constant, does not vary much within the range that is important for the integral.

In the cases, we shall examine, the effect is due to a limited initial disturbance and the salient features are due to the circumstance that $\phi(k)$ has well-defined maxima; thus the prominent part of the effect can be expressed in the form of simple groups belonging to the neighbourhood of the maxima.

Before considering in detail special cases with assigned forms of the velocity function *c*, two illustrations of interest may be mentioned.

We now consider surface waves on an unlimited sheet of deep water, the only bodily forces being those due to gravity. Let the *x*-axis be in the

undisturbed horizontal surface, and the *y*-axis be drawn vertically upwards. Let η be the elevation of surface waves of small amplitude with parallel crests and troughs perpendicular to the *xy*-plane. It can be shown that for an initial displacement given by $\eta = \cos(kx)$, without initial velocity, the surface form at any subsequent time is given by

$$\eta = \cos(kct)\cos(kx) = \frac{1}{2}\{\cos[k(x - ct)] + \cos[k(x + ct)]\},$$

where[†]

$$c = \sqrt{g/k}. \tag{3.7}$$

Let $f(x)$ be any even function of *x* which can be analyzed by Fourier's integral theorem. Then, corresponding to an initial surface displacement $f(x)$, without initial velocity, there is a surface form given at any subsequent time by

$$\eta = \frac{1}{2\pi}\int_0^\infty \phi(k)\cos[k(x - ct)]dk + \frac{1}{2\pi}\int_0^\infty \phi(k)\cos[k(x + ct)]dk, \tag{3.8}$$

where

$$\phi(k) = \int_{-\infty}^{\infty} f(\omega)\cos(k\omega)d\omega. \tag{3.9}$$

If we suppose the initial elevation to be limited practically to a line through the origin and assume that

$$\int_{-\infty}^{\infty} f(x)dx = 1$$

so that $\phi(k) = 1$, we can use, as an illustration of the procedure, the form

$$\eta = \frac{1}{2\pi}\int_0^\infty \cos[k(x - ct)]dk + \frac{1}{2\pi}\int_0^\infty \cos[k(x + ct)]dk. \tag{3.10}$$

[†]We have assumed $c \equiv c_r$, but in the subsequent developments we shall consider a more general case where $c = c_r + ic_i$.

We select from these integrals the groups which give the chief regular features at large distances from the original disturbance. This cumulative group from the first integral is given for a given position and time by the value of k for which $k(x - ct)$ is stationary, where c is given by (3.7), so that

$$\frac{x}{t} = c_g = \frac{1}{2}\sqrt{g/k};$$

and, similarly, from the second integral, we obtain

$$-\frac{x}{t} = \frac{1}{2}\sqrt{g/k}.$$

Thus there are symmetrical groups of waves proceeding in the two directions from the origin; for x positive we need only consider the first integral in (3.10) and for x negative the second integral. Thus the predominant wavelength at a point x at time t is given by

$$k = gt^2/4x^2. \tag{3.11}$$

Evaluating this predominant group, we obtain the well known result

$$\eta = \frac{g^{1/2}t}{2\pi^{1/2}x^{3/2}}\cos\left(\frac{gt^2}{4x} - \frac{\pi}{4}\right). \tag{3.12}$$

At a given position, far enough from the source for the train to be taken as unlimited, this indicates oscillations succeeding each other with continually increasing frequency and amplitude; also if we follow a group of waves with given value of k the amplitude varies inversely as $t^{1/2}$, or inversely as the square root of x.

Accordingly, we shall consider the wave group

$$y = a_1\cos(k_1x - \omega_1t) + a_1\cos(k_2x - \omega_2t)$$

$$= a_2\cos(K_1x - \Omega_1t) + a_2\cos(K_2x - \Omega_2t),$$

where $a_1 \equiv a$; $a_2 = \frac{1}{2}a^2k$; $k_1 \equiv k$; $k_2 \equiv k + \delta k$ $(\delta k \ll 1)$; $K_1 \equiv 2k$; $K_2 \equiv$

$2(k+\delta k)$; $\Omega_1 \equiv 2\omega$; $\Omega_2 \equiv 2(\omega+\delta\omega)$. Using the addition formula for, we obtain

$$y = \left\{2a_1 \cos\left[\frac{1}{2}(\delta k x - \delta\omega t)\right]\right\}\cos\left[\frac{1}{2}(k_1+k_2)x - \frac{1}{2}(\omega_1+\omega_2)t\right]$$

$$= \{2a_2\cos(\delta k x - \delta\omega t)\}\cos\left[\frac{1}{2}(K_1+K_2)x - \frac{1}{2}(\Omega_1+\Omega_2)t\right]. \quad (3.13)$$

The factors in curly brackets are very slowly varying amplitudes (with corresponding amplitudes $\frac{1}{2}(k_2-k_1)$ and (k_2-k_1)). Thus the ratio of the amplitudes gives

$$\frac{a_2\cos(\delta k x - \delta\omega t)}{a_1\cos\frac{1}{2}[\delta k x - \delta\omega t]} \doteqdot \frac{\frac{1}{2}a^2 k}{a} = \frac{1}{2}ak$$

which is of the order of the steepness of the primary wave. Hence, to an observer moving with velocity c_g the profile (3.13) appears to be approximately a train of unsteady Stokes wave (see Figures 1 and 2)[†]

$$y = a\cos(kx) + \frac{1}{2}a^2 k\cos(2kx) \quad (3.14)$$

with the understanding that in the final analysis the amplitude of (3.14) will *not* be assumed constant. In fact, the amplitude $a = \exp(kc_i t)$, where its spatial variation with respect to x is negligible. In what follows we shall refer to c as the group velocity instead of the more commonly used symbol $c_g = c/2$.

3.2. Wave tank experiment

The experiment, reported here, in order to support the fact that as waves

[†]Note that, the 'unsteady Stokes waves' therein are to be interpreted as 'fully nonlinear Stokes waves.' But the second or third order Stokes waves are those that their amplitude is constant.

become sharp-crested (namely, nonlinear Stokes waves) they form a group of waves was performed in our Nonlinear Wave Laboratory. The detail of the experiment is briefly stated below.

We used the wave tank filled with water of depth $h = 0.76\,\mathrm{m}$; the width of the wave tank is 1.2 m. In this experiment, waves were generated at one end of the 12.1 m long wave tank by a vertical piston wave-maker with horizontal motion. Also, for the wind, blowing over the water surface, a fan rotating at 780 RPM (13.2 Hz rotation) with 46 blades and 900 mm diameter is used. The power of this fan is 0.5 HP and thus produces wind at 26 m/s. The piston motion was periodic in a rectangular time profile (namely, step function oscillations) with period $T = 1.4$ seconds and linear amplitude of 0.25 m. Thus, the generated wave traveled along the tank and reflected on the other rigid end, almost without any loss. The combination between direct and reflected waves created a very random type of water surface. Occasionally (for example every 20 seconds or so), some steep waves with angular spike-like profile occurred. These sharp-crested waves had amplitude between 0.22-0.34 m, wavelength in the range 0.2-0.4 m and were rather locally oscillating, standing oscillations, and not really traveling. Some photographs of these waves are depicted in Figures 2(a)-(c). As can be seen from these photographs, these waves eventually become sharp-crested which are composed of wave groups. Hence, this relatively simple experiment demonstrates that initial Stokes waves, travelling far enough become unstable and eventually form a group. It should be noted this phenomenon is attributed to wave-wave interactions between two harmonics of the wave. Thus, this experiment supports our theory of formation of wave groups, as outlined in the previous section.

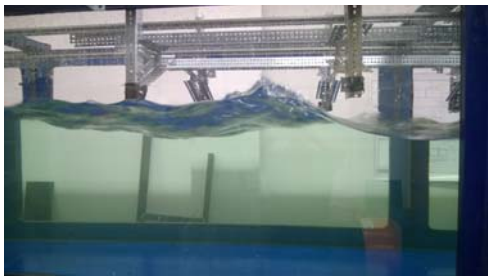

(a)

(b)

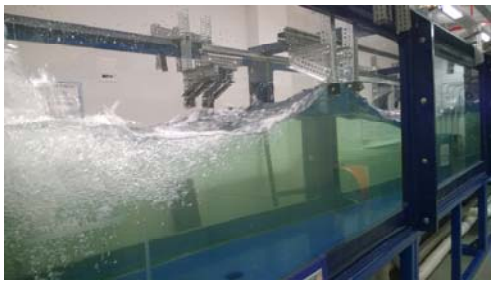

(c)

Figure 2. Water tank experimental evidence showing as nonlinear waves propagate it becomes unstable and forms a sharp-crested wave. The formation of a wave group for sharp-crested wave can easily be seen in the downstream of the wave. The water depth $h = 0.76\,\mathrm{m}$, the wave tank is $1.2\,\mathrm{m}$ wide and $12.1\,\mathrm{m}$ long. Waves were generated at one end of the tank wave tank by a vertical piston wave-maker with horizontal motion. The piston motion is periodic in a rectangular time profile with period $T = 1.4$ seconds and amplitude of $0.25\,\mathrm{m}$. These sharp-crested waves have amplitude between 0.22-$0.34\,\mathrm{m}$, wavelength in the range 0.2-$0.4\,\mathrm{m}$.

4. Airflow over Wave Group

With reference to Figures 1 and 2, we choose, as independent variables, the coordinates s and n measured along and normal to the streamlines (see Figure 3) in a frame of reference moving with the wave speed c_r and, as dependent variables $q(s, n)$ and $\theta(s, n)$, the velocity along a streamline and the inclination of the streamline, respectively. We begin with the intrinsic equations of motion (Milne-Thomson [34, Section 21.39])

$$q\frac{\partial q}{\partial s} + \frac{1}{\rho}\frac{\partial p}{\partial s} = \nu\frac{\partial^2 q}{\partial n^2}, \tag{4.1a}$$

$$q^2\frac{\partial \theta}{\partial s} + \frac{1}{\rho}\frac{\partial p}{\partial n} = 0, \tag{4.1b}$$

$$\frac{\partial q}{\partial s} + q\frac{\partial \theta}{\partial n} = 0, \tag{4.1c}$$

where ρ denotes density, p hydrodynamic pressure, ν kinematic viscosity (all parameters in this section referring to the air), and the right-hand side of (4.1a) represents the dominant shear term in a boundary-layer-type approximation. We shall seek the perturbation flow coupled with the unsteady Stokes wave

$$\eta(s) = a(t)e^{iks} + \frac{1}{2}a^2(t)ke^{2iks} \equiv \eta_1 + \eta_2 \tag{4.2}$$

on $n = 0$ in a uniform, parallel shear flow $q^{(0)} = U(n) - c_r$ (with understanding that the imaginary parts of complex quantities are proportional to $\exp(iks)$ and $\exp(2iks)$.) The final motion will be unstable if $\mathscr{I}\{c\} > 0$, exhibiting the time-growth factor $\exp(k\mathscr{I}\{c_r\}t)$.

We first note that the unperturbed solution to (4.1a, b, c) implied by our assumption of a strictly parallel shear flow is

$$q = q^{(0)}(n), \quad p = p^{(0)}(s), \quad \theta \equiv 0. \tag{4.3a, b, c}$$

In fact, we shall use (4.1a, b, c) to describe perturbations with respect to a turbulent flow for which $U(n)$ is the mean flow and in which the viscous stress $\rho\nu U'$ is actually balanced by a Reynolds stress; the model provided by (4.1a, b, c) then neglects perturbation Reynolds stresses.

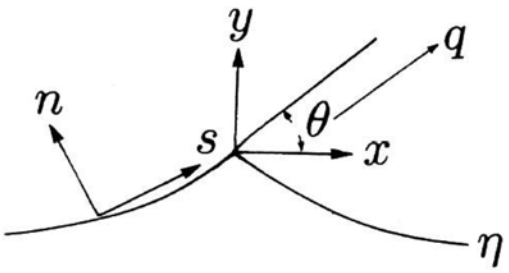

Figure 3. The coordinates for the intrinsic equations of motions (2.1a, b, c).

We may linearize (4.1a, b, c) in the independent variable $\theta(s, n)$ by differentiating (4.1a) with respect to both s and n and (4.1b) twice with respect to s, taking the difference between the results to eliminate p, and eliminating q_s through (4.1c) to obtain

$$\frac{\partial}{\partial s}\left[\frac{\partial}{\partial n}\left(q^2\frac{\partial\theta}{\partial n}\right)+\frac{\partial}{\partial s}\left(q^2\frac{\partial\theta}{\partial s}\right)\right]=\nu\frac{\partial^3}{\partial n^3}\left(q\frac{\partial\theta}{\partial n}\right). \tag{4.4}$$

Now, to first order in θ, we may approximate q by its undisturbed value $U(n)-c$ and assume θ to exhibit the harmonic s-dependent of the form

$$\theta(s, n)=e^{iks}\Theta_1(n)+ake^{2iks}\Theta_2(n) \tag{4.5}$$

to obtain

$$\frac{\partial}{\partial n}(q^2\Theta_1')-k^2(q^2\Theta_1)=\frac{\nu}{ik}\frac{\partial^3}{\partial n^3}(q\Theta_1') \tag{4.6}$$

and

$$\frac{2}{k}\frac{\partial}{\partial n}(q^2\Theta_2')-8k(q^2\Theta_2)=\frac{\nu}{ik}\frac{\partial^3}{\partial n^3}(q\Theta_2') \tag{4.7}$$

as the linearized equation of motion for $O(a)$ and $O(a^2)$, respectively. We

remark that (4.6) differs from a boundary-layer approximation to the Orr-Sommerfeld equation (governing the perturbation stream function in Cartesian coordinates) in that it has a singularity at $U = c$; this implies that the linearized approximation to θ cannot be uniformly valid in the neighbourhood of $U = c$.[†] We shall find that this singularity introduces no essential difficulty (in so far as we require only the perturbation stresses at the interface $n = 0$), but it should be distinguished from the singularity that occurs at $U = c$ for the inviscid Orr-Sommerfeld equation of (4.11a) below; the latter singularity is a consequence of neglecting the viscous forces in a neighbourhood where the inertial forces tend to zero (cf. SHD).

We shall present the full boundary condition in Section 6 below, but we note that

$$\theta(0, s) = \eta'(s) \text{ and } \theta \to 0 \text{ as } n \to \infty. \qquad (4.8a, b)$$

Note that these boundary conditions are imposed at the displaced, rather than the mean, position of the interface, thereby avoiding the assumption that the surface-wave displacement η must be small compared with a characteristic length (say c/U') for the shear profile; thus, we have only to assume $k|\eta| \ll 1$, rather than $U'(0+)|\eta|/c[= S_a k|\eta|] \ll 1$. It is for this reason that we choose a formulation in terms of $\theta(s, n)$, the streamline inclination in non-Cartesian coordinates, rather than the more conventional formulation in terms of a stream function in Cartesian coordinates.

We shall seek asymptotic solution to (4.6) and (4.7) in the limit as $R = c/k\nu \to \infty$. The formal procedure is essentially the same as that for the Orr-Sommerfeld equation (see Lin [24, Sections 3.4 and 3.6]) and yields two solutions for both equations (4.6) and (4.7) which satisfy the boundary condition (4.8b). The first of these, the *inviscid solution*, may be obtained by setting $\nu = 0$ in (4.6) and (4.7); the second or *viscous solution*, may be

[†]In our earlier calculations, Croft and Sajjadi [9], formulation in orthogonal curvilinear coordinates avoided this difficulty. However, that formulation led to an inhomogeneous form of the Orr-Sommerfeld equation unless terms in U^{iv} and U''' were neglected.

obtained by neglecting the second term on the left-hand side of (4.6) and (4.7) or equivalently, omitting the pressure gradient in (4.1a) and disregarding (4.1b). We find it convenient to solve for $(U-c)\theta$ and $(U-c)\theta_n$ (which are proportional to vertical velocity and perturbation shearing stress) in these two cases and to separate the *s*-dependence by introducing the factor $\eta'(s)$; defining the dimensionless variables

$$\xi = kn, \quad f(\xi) = [U(n) - c]/c \tag{4.9a, b}$$

we then express $\Theta_i(n)$ as an inviscid plus viscous contributions in the form

$$\Theta_i(n) = \hat{\Theta}_i(n) + \tilde{\Theta}_i, \quad i = 1, 2, \tag{4.10a}$$

where

$$f(\xi)\hat{\Theta}_i(n) = -ik\phi_i(\xi), \quad f(\xi)\tilde{\Theta}_i'(n) = -ik^2\chi(R^{1/2}\xi), \tag{4.10b, c}$$

$$\Theta_i(n) = -ika\left[\frac{\phi_i(\xi)}{f(\xi)} + \int_\infty^\xi \frac{\chi_i(R^{1/2}\xi)d\xi}{f(\xi)}\right] \tag{4.10d}$$

and

$$f\phi_i'' - (f'' + f)\phi_i = 0, \tag{4.11a}$$

$$\frac{d^2\chi_i}{d\xi^2} - iRf\chi_i = 0 \text{ or } \chi_i'' - iRf\chi_i = 0 \tag{4.11b, c}$$

as may be confirmed either by substituting (4.10d) in (4.6) and (4.7) and allowing *R* to tend to infinity or through the approximation described in the proceeding sentence.

The inviscid equation (4.11a) is identical with the inviscid Orr-Sommerfeld equation, which shows that our introduction of intrinsic coordinates and the imposition of the boundary condition (4.8a) at the displaced position of the interface have not altered the inviscid problem. The viscous equation (4.11b), on the other hand, differs from its counterpart in the asymptotic solution of the Orr-Sommerfeld equation in consequence of

our choice of variables. However, the methods of asymptotic solution remain the same and, we may use the WKB approximation (Sajjadi [39]) to obtain

$$\chi_1 \sim f^{-1/4} \exp\left\{-\int_{\xi_c}^{\chi} \sqrt{iRf}\, d\xi\right\}[1 + O(R^{-1/2})], \tag{4.12a}$$

$$\chi_2 \sim f^{-1/4} \exp\left\{-\int_{\xi_c}^{\chi} \sqrt{2iRf}\, d\xi\right\}[1 + O(R^{-1/2})], \tag{4.12b}$$

where $f(\xi_c) = 0$ and the phase of the radical in (4.12a) or (4.12b) is $\pm\frac{1}{4}\pi$ as $\xi \gtrless \xi_c$, the path of integration being indented under the branch point at $\xi = \xi_c$ (Lin [24, Section 3.4]). Note also that the error factor in (4.12a) and (4.12b) is referred to the exact solution of (4.6) and (4.7), respectively, and not to (4.11a).

Furthermore, it should be noted that neither (4.12a) nor (4.12b) are uniformly valid near $\xi = \xi_c$, but they suffice for the present purpose in so far as $S \ll R^{1/2}$ (the condition that the inner and outer viscous layers be well separated), a condition that will be satisfied for those combinations of parameters for which viscous dissipation in the air is most significant (albeit still small).

It now remains to express the perturbation stresses on the interface in terms of ϕ_i and χ_i. Neglecting terms $O(R^{-1})$, in keeping with the present boundary-layer approximation, we may calculate the normal stress from (4.1a), (4.3a, b), (4.10) and (4.11b) according to

$$p^{(nn)} = -e^{iks}(P_1 - P_1^{(0)}) - ake^{2iks}(P_2 - P_2^{(0)}) \tag{4.13a}$$

$$= -(ik)^{-1}\rho[\Theta_1' q^2 - (\nu/ik)(q\Theta_1')_{nn}]e^{iks}$$

$$- (2ik)^{-1}\rho[\Theta_2' q^2 - (\nu/2ik)(q\Theta_2')_{nn}]ake^{2iks} \tag{4.13b}$$

$$= \rho c^2 k\{[f\phi_1'(0) - f'\phi_1(0)]\eta_1 + [f\phi_2'(0) - f'\phi_2(0)]\eta_2\}. \tag{4.13c}$$

Evaluating (2.13c) at $n = 0$, where $f = -1$ and $f' = S$ since

$$S_a = U'(0+)/kc = U_*^2/kc\nu_a = R_a(U_*/c)^2,$$

we may write

$$(p^{(nn)})_{n=0+} = -\rho c^2 k[\varpi_1\eta_1\phi_1(0) + \varpi_2\eta_2\phi_2(0)], \tag{4.14}$$

where

$$\varpi_j = \frac{\phi_j'(0)}{\phi_j(0)} + S = (\alpha_j + i\beta_j)\left(\frac{U_1}{c}\right)^2, \quad j = 1, 2 \tag{4.15a, b}$$

the parameter α_j and β_j are related to the resulting pressure which acts on the boundary (where $\phi_j(0) = 1$)

$$p = \rho U_1^2 k\sum_{n=1}^{\infty}(\alpha_n + i\beta_n)\eta_n \tag{4.15c}$$

and the argument zero implies evaluation at $\xi = 0+$. Note that the results given (4.14) and (4.15a, b) for second-order Stokes wave can be generalized for higher-order Stokes wave in much the same way without difficulty. For example, for third-order Stokes wave

$$\eta = ae^{iks} + \frac{1}{2}a^2ke^{2iks} + \frac{3}{8}a^3k^2e^{3iks} \equiv \eta_1 + \eta_2 + \eta_3,$$

(4.13) and (4.14) become

$$\begin{aligned} p^{(nn)} &= -(ik)^{-1}\rho[\Theta_1'q^2 - (\nu/ik)(q\Theta_1')_{nn}]e^{iks} \\ &\quad - (2ik)^{-1}\rho[\Theta_2'q^2 - (\nu/2ik)(q\Theta_2')_{nn}]ake^{2iks} \\ &\quad - (3ik)^{-1}\rho[\Theta_3'q^2 - (\nu/3ik)(q\Theta_3')_{nn}]a^2k^2e^{3iks} \end{aligned} \tag{4.16a}$$

$$\begin{aligned} &= \rho c^2 k\{[f\phi_1'(0) - f'\phi_1(0)]\eta_1 \\ &\quad + [f\phi_2'(0) - f'\phi_2(0)]\eta_2 + [f\phi_3'(0) - f'\phi_3(0)]\eta_3\} \end{aligned} \tag{4.16b}$$

and where (4.16b) is evaluated at $n = 0,$ we obtain

$$(p^{(nn)})_{n=0+} = -\rho c^2 k[\varpi_1\eta_1\phi_1(0) + \varpi_2\eta_2\phi_2(0) + \varpi_3\eta_3\phi_3(0)]. \quad (4.17)$$

Thus for higher-order Stokes wave (4.14) and (4.15) generalize to

$$(p^{(nn)})_{n=0+} = -\rho k^2 c^2 \sum_{j=1}^{\infty}\left(\frac{\phi_j'(0)}{\phi_j(0)} + S\right)\eta_j$$

$$= -\rho k c^2\left(\frac{U_1}{c}\right)^2 \sum_{j=1}^{\infty}(\alpha_j + i\beta_j)\eta_j. \quad (4.18a, b)$$

The expressions (4.18) are in full agreement with earlier works of Sajjadi and co-workers.

The tangential stress is given by (within the boundary-layer approximation)

$$p^{(sn)} = \rho\nu(q_n - U') \quad (4.19a)$$

$$= (-ik)^{-1}\rho\nu[q(\Theta_1'\eta_1 + \Theta_2'\eta_2)]' \quad (4.19b)$$

$$= \rho c^2 R^{-1/2}[\chi_1'(R^{1/2}\xi)k\eta_1 + \chi_2'(R^{1/2}\xi)k\eta_2]. \quad (4.19c)$$

Substituting χ_i from (4.12) and setting $\xi = 0+,$ we obtain

$$(p^{(sn)})_{n=0+} = -e^{\pi i/4}\rho c^2 R^{-1/2}[\chi_1(0)k\eta_1 + \sqrt{2}\chi_2(0)k\eta_2]. \quad (4.20)$$

Note that the viscous solution enters the calculation of the normal stress and the inviscid solution that of the tangential stress only through the boundary conditions, which relate $\phi_i(0)$ and $\chi_i(0)$.

5. Equations of Motion for Group of Waves

We shall now proceed on the assumption that the shear flow in the water (which is induced by the traction of the shear flow in the air) may be neglected. As was stated in Section 1, this will be a good approximation if

$S_w \ll 1$, where S_w is defined by (1.4). We must stress at this point that this assumption does not preclude the existence of a surface current, since our velocities are defined relative to such a current; all that $S_w \ll 1$ implies is that the water moves approximately uniformly with the surface current to a depth of the order $1/k(= \lambda/2\pi)$. In addition to this, the small shear flow that is present must be oppositely directed to the airflow, for example $U_w < 0$ if $U_a > 0$; it follows that $U - c_r$ could not vanish in $n < 0$ for wave traveling downwind, whence the shear flow in the water could not transfer energy to the surface wave through the critical layer mechanism. Note that such an energy transfer would be predicted for a wave traveling upwind, but it generally would be much smaller than the energy absorbed by viscous dissipation, primarily because $U_w \ll 1$ at the depth where $U_w - c_r = 0$.

Assuming small perturbations with respect to a uniform flow –*c* (relative to the moving frame of reference), we follow Lamb [22, Section 349] and construct a solution for a surface wave of the form (4.2) moving over a viscous liquid. If we omit the hydrodynamic static pressure from $P^{(nn)}$ and note that $v = -c\theta$, we may pose the streamline inclination and perturbation stresses in the forms

$$\theta = (a_1 e^{\xi} + b_1 e^{\kappa\xi}) ik\eta_1 + (a_2 e^{\xi} + b_2 e^{\kappa\xi}) ik\eta_2, \tag{5.1}$$

$$\begin{aligned} p^{(nn)} &= -\rho c^2 [(1 + 2iR^{-1}) a_1 e^{\xi} + 2i\kappa R^{-1} b_1 e^{\kappa\xi}] k\eta_1 \\ &\quad - \rho c^2 [(1 + 2iR^{-1}) a_2 e^{\xi} + 2i\kappa R^{-1} b_2 e^{\kappa\xi}] k\eta_2, \end{aligned} \tag{5.2}$$

$$\begin{aligned} p^{(sn)} &= \rho c^2 [2R^{-1} a_1 e^{\xi} + (2R^{-1} - i) b_1 e^{\kappa\xi}] k\eta_1 \\ &\quad - \rho c^2 [2R^{-1} a_2 e^{\xi} + (2R^{-1} - i) b_2 e^{\kappa\xi}] k\eta_2, \end{aligned} \tag{5.3}$$

$$\kappa = (1 - iR)^{1/2}, \quad \mathscr{R}\{\kappa\} > 0, \tag{5.4a, b}$$

where a_i and b_i are constants to be determined by the boundary conditions at the interface, and ρ, ν, and R are to be evaluated for the water. Note that

the boundary-layer approximation is not applicable to the water (since the interface is approximately free for the heavy fluid below the interface) and that (5.1)-(5.4) are based on the full, linearized equations of viscous flow; subsequently, we shall assume $R_w \gg 1$, but this approximation has yet to be invoked.

6. Energy Transfer to Group of Waves

In order to evaluate the energy transfer from shear flow to Stokes wave we must first proceed with determination of wave speed. Thus, we may infer the boundary conditions at the interface from the considerations that both θ_a and θ_w must be equal to the slope of the surface wave, that the velocity (or θ_n) be continuous, that the shear stress be continuous, and that the discontinuity in normal stress be prescribed. Accordingly

$$\theta_a = ik\eta, \quad \theta_w = ik\eta, \quad \Delta\theta_n = 0, \tag{6.1a, b, c}$$

$$\Delta p^{(sn)} = 0, \quad \Delta p^{(nn)} = L\eta, \tag{6.1d, e}$$

where

$$\Delta(\ ) = (\ )_{n=0+} - (\ )_{n=0-} \tag{6.2}$$

and $L\eta$ the (static) restoring viscous stress of the interface. We may relate the operator L to the inviscid wave speed in the absence of the upper-fluid according to

$$L\eta = \rho_w c_w^2 k\eta \tag{6.3}$$

which for second-order Stokes gravity waves is given by

$$c_w^2 = gk^{-1}(1 + k^2a^2) = c_{w0}^2 + c_{w1}^2. \tag{6.4}$$

We note that for group of waves $(c_w)_g = c_w/2$. Moreover, we need not pose the boundary conditions at infinity, assuming them to be satisfied implicitly.

Substituting (4.10d), (4.14), (4.20), (5.1)-(5.3) and (6.3) in (6.1a-e),

setting $f(0) = -1$ and $f'(0) = S_a$, and canceling common factors, we may place the results in the form

$$\phi_1(0) - e^{\pi/4} R_a^{-1/2} \chi_1(0) = 1, \tag{6.5a}$$

$$\phi_2(0) - e^{\pi/4} R_a^{-1/2} \chi_2(0) = \frac{1}{2}, \tag{6.5b}$$

$$a_1 + b_1 = 1, \tag{6.5c}$$

$$a_2 + b_2 = 1, \tag{6.5d}$$

$$\phi_1'(0) + S_a \phi_1(0) + \chi_1(0) = a_1 + \kappa b_1, \tag{6.5e}$$

$$\phi_2'(0) + S_a \phi_2(0) + \chi_2(0) = \frac{1}{2}(a_2 + \kappa b_2), \tag{6.5f}$$

$$-e^{-\pi i/4} \sigma R_a^{-1/2} \chi_1(0) = 2R_w^{-1}(a_1 + b_1) - i b_1, \tag{6.5g}$$

$$-e^{-\pi i/4} \sigma R_a^{-1/2} \chi_2(0) = \frac{2}{\sqrt{2}} R_w^{-1}(a_2 + b_2) - i b_2, \tag{6.5h}$$

$$c_{w0}^2 = c_0^2[(1 + 2iR_w^{-1})a_1 + 2i\kappa R_w^{-1} b_1 - \sigma \varpi_1 \phi_1(0)], \tag{6.5i}$$

$$c_{w1}^2 = c_1^2[(1 + 2iR_w^{-1})a_2 + 2i\kappa R_w^{-1} b_2 - \sigma \varpi_2 \phi_2(0)], \tag{6.5j}$$

where c_0 and c_1 are complex. Solving (6.5a-j) for $\phi_i(0)$, $\chi_i(0)$, a_i and b_i, $i = 1, 2,$ and substituting in (6.5i) and (6.5j), we obtain

$$\begin{aligned} c^2 &= c_0^2 + c_1^2 \\ &= c_{w0}^2[\mathscr{F}_1 + k^2 a^2 \mathscr{F}_2] + O[R_w^{-3/2}, \sigma R_a^{-1/2} R_w^{-1/2}, \sigma S_a R_a^{-1}, \sigma^2], \end{aligned} \tag{6.6}$$

where

$$\mathscr{F}_1 = 1 - 4iR_w^{-1} + \sigma \varpi_1 - \sigma(1 - \varpi_1)^2 e^{\pi i/4} R_a^{-1/2}$$

and

$$\mathscr{F}_2 = 1 - (2 + \sqrt{2}) iR_w^{-1} + \sigma \varpi_2 - \sigma(1 - \varpi_2)^2 e^{\pi i/4} R_a^{-1/2}.$$

Substituting φ_i from (4.15b) and R_w and R_a from (1.3b) in (6.6) and neglecting higher-order terms, we obtain the damping ratio for unsteady Stokes wave

$$\zeta = kc_i = \frac{2\mathscr{I}\{c\}}{\mathscr{R}\{c\}} = \underbrace{\sigma\beta_1\left(\frac{U_1}{c_r}\right)^2}_{\text{(i)}} \underbrace{- \frac{4g\nu_w}{c_r^3}}_{\text{(ii)}}$$

$$\underbrace{- \sigma\left(\frac{g\nu_a}{2c_r^3}\right)^{1/2}\left[1 - 2(\alpha_1 + \beta_1)\left(\frac{U_1}{c_r}\right)^2 + (\alpha_1^2 + 2\alpha_1\beta_1 - \beta_1^2)\left(\frac{U_1}{c_r}\right)^4\right]}_{\text{(iii)}}$$

$$\underbrace{+ \sigma\beta_2\left(\frac{U_1}{c_r}\right)^2}_{\text{(iv)}} \underbrace{- \frac{(2+\sqrt{2})g\nu_w}{c_r^3}}_{\text{(v)}}$$

$$\underbrace{- \sigma\left(\frac{g\nu_a}{2c_r^3}\right)^{1/2}\left[1 - 2(\alpha_2 + \beta_2)\left(\frac{U_1}{c_r}\right)^2 + (\alpha_2^2 + 2\alpha_2\beta_2 - \beta_2^2)\left(\frac{U_1}{c_r}\right)^4\right]}_{\text{(vi)}}, \tag{6.7}$$

where the terms (i)-(iii) on the right-hand side represent, respectively, the positive energy transfer from the shear flow, the viscous dissipation in the water, and the viscous dissipation in the air for the fundamental harmonic (being exactly the same as that for a monochromatic wave provided c_r is replaced with $\sqrt{g/k}$), whereas terms (iv)-(vi) represent the same for the second harmonic.

7. Application of the Theory to Spectral Wave Models

Spectral wave models, such as WAM, describe the evolution of a two-dimensional ocean wave variance spectrum through integration of the transport equation

$$\frac{D\mathsf{F}}{Dt} + \frac{\partial}{\partial \varphi}(\dot{\varphi}\mathsf{F}) + \frac{\partial}{\partial \mu}(\dot{\mu}\mathsf{F}) + \frac{\partial}{\partial \vartheta}(\dot{\vartheta}\mathsf{F}) = \mathsf{S},$$

where F represents the spectral density with respect to directions ϑ, latitudes φ and longitudes μ (the dot over symbols denotes the rate of change of the position and propagation of a wave packet).

The source function S is represented as a superposition of the wind input S_{in}, white capping dissipation S_{dis}, and nonlinear transfer S_{nl}, i.e.,

$$\mathsf{S} = \mathsf{S}_{\text{in}} + \mathsf{S}_{\text{dis}} + \mathsf{S}_{\text{nl}}.$$

Here, we shall only be concerned with S_{in} and offer an alternative formulation of it.

The wind input is usually given by

$$\mathsf{S}_{\text{in}} = \zeta \mathsf{F},$$

where ζ represents the growth rate of the waves. According to Miles [29] mechanism, the growth rate, when normalized with frequency ω, is given by (1.2). In the third generation model of WAM, the energy transfer parameter appearing in (1.2), taken from the asymptotic expression derived by Janssen [16, 17], is given by

$$\beta_{\text{asym}} = \frac{\beta_m}{\kappa^2} ky_c \ln^4(ky_c), \quad ky_c < 1, \tag{7.1}$$

where now κ is the von Kármán's constant, $\beta_m = 1.2$ a constant and

$$ky_c = \min(1, ky_0 e^{\kappa/(U_*/c_r + 0.011)})$$

is the dimensionless critical height.

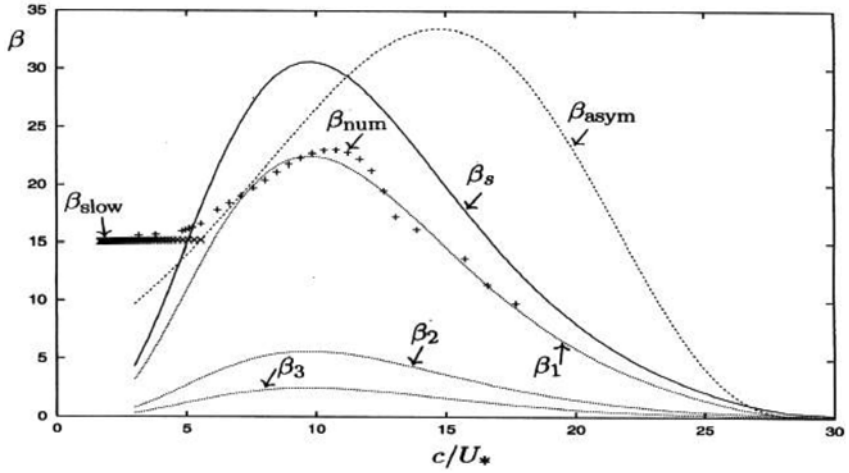

Figure 4. The plot of β against c/U_*. Dotted line (…) is the result obtained by the present model for the first three harmonics of Stokes wave, pluses (+) are numerical results of Sajjadi [43], crosses (×) are the numerical results obtained by Sajjadi [43] for slow moving waves, solid line (–) is the result obtained by the present model for a third-order Stokes wave, and the dashed line (---) is Janssen's [17] asymptotic result.

We shall now apply the foregoing theory to the growth of water waves (Stokes and group of sharp-crested) by wind on the hypothesis that the air mean velocity in the turbulent boundary layer may be regarded as parallel shear flow. We shall assume that the mean velocity profile in the vicinity of the air-water interface is asymptotically logarithmic according to

$$U(n) = \frac{U_*}{\kappa} \log(n/n_0), \tag{7.2}$$

where U_* is the wind friction velocity and κ is Kármán's constant. We perform calculations for waves with wavelength $\lambda = 0.64\,\text{m}$, and initial wave steepness $a_0 k = 0.01$, where a_0 is the initial wave amplitude. We choose the value of $kn_c = 10^{-4}$ for the non-dimensional roughness length and evaluate the energy transfer parameter over a range of c_r/U_*. For growing waves we fix the value of waves complex speed to $c_i = 0.1$.

In Figure 4, we have plotted the expression for β_{asym}, given by (7.1), as a function of c_r/U_* (the dashed line). As can be seen from this figure the peak value of β_{asym} is approximately 34 which occurs at $c_r/U_* = 16$. Also in Figure 4 we have plotted β calculated with the present numerical integration of the Orr-Sommerfeld equation for the first 3 harmonics of Stokes wave, namely $\beta_i,\ i = 1, 3$ (the dotted lines). Note incidentally that β_1 corresponds to the monochromatic wave and the results obtained by Janssen [16, 17] (also for monochromatic waves) leads to growth rate that is a factor of

$$O\left(\frac{\kappa^{-1}\ln(\lambda n_0)}{1 + c_r/U_*}\right)$$

too large compared to the growth rate obtained from β_1. As can be seen from this figure β_1 agrees very well with β_{num} (pluses), obtained from the numerical integration of full Reynolds stress transport equations over water waves using the two-component limit of turbulence (TCL) (Sajjadi and Drullion [47]), over the range $7 \le c_r/U_* \le 18$. However, in the range $2 \le c_r/U_* \le 5$ both the present model and the asymptotic theory of Janssen [16, 17] fails to capture the saturated trend of β. This is not surprising since neither of these models take into account the implicit nature of turbulence other than in prescribing the logarithmic mean wind velocity profile over the surface wave. It can be seen that β tends to an approximately constant value of 15 in the range $2 \le c_r/U_* \le 7$, being the range in which U_* is large (normally referred to as the slow moving wave regime). We observe that the numerical simulation, using the TCL model, captures the behavior of β in this range and hence qualitatively agrees with the asymptotic result of Belcher and Hunt [1].

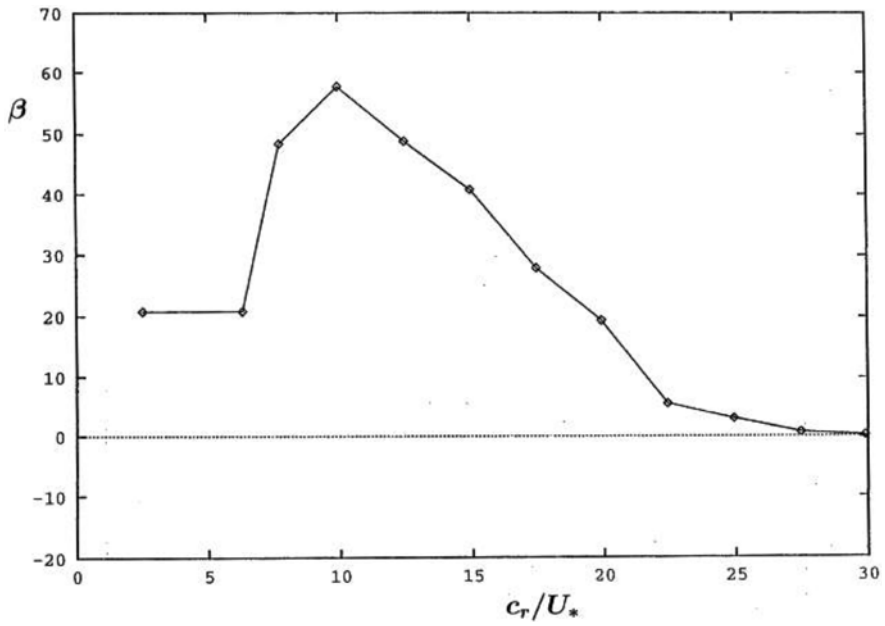

Figure 5. Variation of the energy-transfer parameter, β, with the wave age c_r/U_* for sharp-crested group of wave.

Recently by invoking a closure model, based on Townsend [56], Sajjadi [46] constructed a model for the specification of turbulent Reynolds stresses over water waves where the resulting equation together with its corresponding boundary conditions was solved numerically. The energy transfer parameter was then calculated from the derived expressions for the momentum flux for slow wind-wave regime $(c_r/U_* \leq 5)$ which agreed well with that of Sajjadi [45]. The results of these calculations are also shown in Figure 4 (crosses), namely β_{slow} for comparison.

Figure 4 also shows the plot of β_s, given by

$$\beta_s = \sum_{n=1}^{N} (ak)^{n-1} \beta_n \tag{7.3}$$

for $N = 3$ which corresponds to energy transfer from wind to a third-order Stokes wave. From (7.3) it is evident that for $a_0 k \ll 1$, $\beta_1 > \beta_2 > \beta_3$ and

thus the increased energy transfer to nonlinear waves is due to the presence of the additional terms, namely β_i, $i \geq 2$, compared to the monochromatic counterpart. Note that in the present calculations, the magnitude of $\beta_4 \ll 1$ and therefore its inclusion to series (7.3) will have an insignificant effect to the overall magnitude of β_s (if *N* was taken to be 4 in series (7.3)).

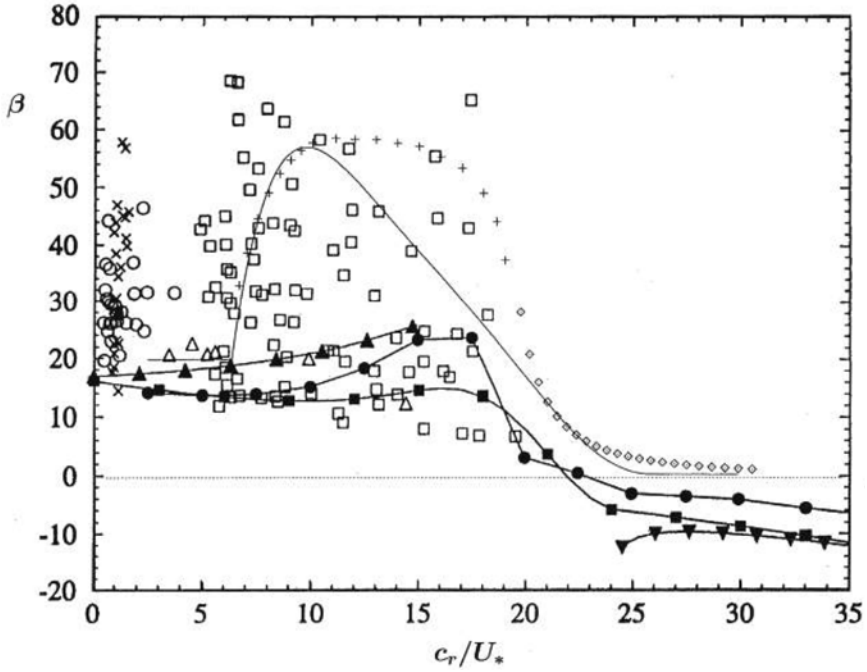

Figure 6. Variation of the energy-transfer parameter, β, with the wave age c_r/U_* for sharp-crested group of wave and Stokes waves with experimental data of Snyder et al. [48]. Thin solid line presents prediction numerically for sharp-crested group of wave; +, presents prediction analytically (small to moderate values of c_r/U_*) for sharp-crested group of wave; ◇, presents prediction analytically (large values of c_r/U_*) for sharp-crested group of waves; ■-■, steady monochromatic waves; ●-●, steady second-order Stokes wave; ▲-▲, asymptotic prediction for unsteady Stokes wave for small to moderate values of c_r/U_*; ▼-▼, asymptotic prediction for unsteady Stokes wave for large values of c_r/U_*. Other symbols are Snyder's data.

Figure 6 shows the variation of β with the wave age c_r/U_* for several models and their comparison with experimental data of Snyder's [48] data. Two important factors can immediately be observed: (i) the numerical solution of β through integration of the Orr-Sommerfeld equation (see the Appendix) agree very well with the numerical solution of TCL model shown in Figure 5. It is important to note the numerical values of β (the thin solid line) qualitatively and quantitatively agree with the results shown in Figure 5; (ii) in both cases the maximum value of $\beta \approx 58$ and this maxima occur at $c_r/U_* \approx 11$. However, for $c_r/U_* \gg 1$ the numerical value of β, shown in Figure 6, does not become negative. Hence, the solution obtained using the Orr-Sommerfeld equation does not seem to capture wave decay for large values of c_r/U_*. Also for comparison asymptotic results obtained for fully nonlinear Stokes waves (Sajjadi [41]) is also shown. It can be seen in two asymptotic regions, where c_r/U_* is small or large, there is a good agreement with present computation, but Sajjadi's [41] theory does not agree with the present computation.

We now focus our attention to unsteady group of sharp-crested waves. In contrast to steady waves (monochromatic and Stokes), the results obtained for group of sharp-crested waves are considerably different. Figure 5 shows the variation of β for group of sharp-crested waves with the wave age c_r/U_*, with a fixed the value of $c_i = 0.1$. The results depicted in Figure 5 is obtained using the TCL model (see Sajjadi and Drullion [47]) in the range $2 \le c_r/U_* \le 30$. As can be seen from this figure the numerical calculations of β predicts the same trend as that of β_{slow} obtained by Belcher and Hunt [1]. However, we also observe that β reaches maximum value of 58 at $c_r/U_* \approx 11$ which is $\frac{1}{2} c_r/U_*$ obtained by numerical simulation of Reynolds stress model obtained by Mastenbroek et al. [28]. But, we emphasize that in their study they considered very small steepness steady waves. We remark that, for $c_r/U_* \gg 1$, beyond $c_r/U_* = 30$ (not shown here), β becomes negative. This implies that sharp-crested group of waves decay much slower

than that of small steepness steady waves, which, from oceanographic view point, is not surprising.

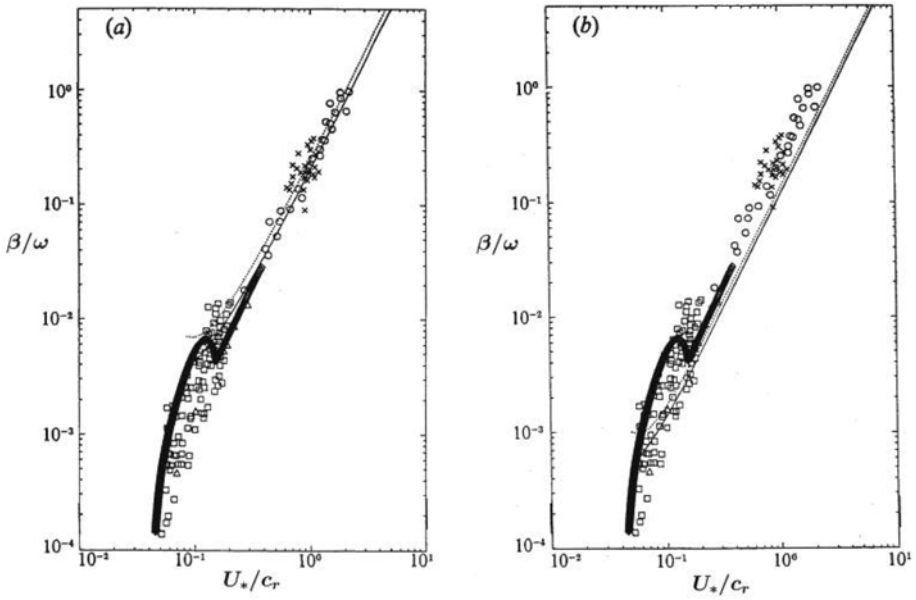

Figure 7. The growth rate of the energy density of the wave (twice the amplitude growth rate) due to the effect of the asymmetric pressure, made non-dimensional on the wave frequency. The thin and dotted lines are the theoretical curves, due to Belcher and Hunt [1], are compared with the data collated by Plant [38]. The thick line represents the present prediction of β for $c_i = 0.1$. The upper group of experimental points is mainly from wave tank experiments and the lower group from oceanic experiments. (a) $\lambda/y_0 = 10^3$ typical of the wave tank experiments, (b) $\lambda/y_0 = 10^5$ typical of the ocean experiments.

Finally, Figures 7(a) and 7(b) show comparisons of the theoretical prediction of the normalized on the frequency of the wave, $\omega = 1/T$, growth rate of the energy transfer parameter, β, together with the laboratory data collated by Plant [38]. In Figure 7(a), λ/y_0 has the value 10^3, which is representative of the laboratory experiments, and in Figure 7(b), λ/y_0, is 10^5,

representative of ocean waves. The result of the present parameterization of β for sharp-crested wave group, with $c_i = 0.1,$ is also plotted.

8. Conclusions

The study undertaken in this paper warrants the following conclusions. We have investigated three important unresolved problems remaining in oceanography in some depth. These include: (a) unsteady waves, where waves are allowed to grow or decay rather than assuming their initial amplitude during their propagation; (b) non-monochromatic waves, which are not characteristic in oceans, and in fact can never be observed; and (c) group of waves, which can often become sharp-crested by receiving enough energy from the wind shear flow as they propagate. The ultimate aim of this investigation was the more in depth understanding the air-sea interactions, taking into account non-ideal and group of waves, in order to improve the parameterization of the energy input from wind to waves which can be incorporated in spectral wave models. In this paper, we have shown the sum of two simple harmonic waves can lead to an unsteady fully nonlinear Stokes waves which can become sharp-crested. Thus, as a starting point we have (i) presented results on the simplest approximation to such wave groups; (ii) imposed the boundary condition at the surface wave, rather than at the mean surface. The latter will be inappropriate as waves tend to become sharp-crested their profile will be well above the mean undisturbed water surface; (iii) assumed the wave phase velocity is complex which consequently allows the wave amplitude to grow or decay according to $a(t) = a_0 e^{kc_i t},$ where a_0 is the initial constant amplitude, k is the wave number, and c_i is the wave complex phase speed. Thus the rate of growth (or decay) such waves $\zeta = kc_i$; and, (iv) include the dominant viscous term in the perturbation equations, similar to that adopted by SHD.

We have found that: (i) yields an energy-transfer coefficient that is larger than that previously calculated for monochromatic waves and agree well with experimental data Snyder et al. [48] and Plant [38], also with the result

obtained by full numerical integration of the Reynolds stress transport equations, performed recently by Sajjadi and Drullion [47]; (ii) has no major effect on the end-results if appropriate number of harmonics is taken into account for nonlinear as well as group of waves; (iii) showed the variation of dimensionless energy-transfer parameter β with the wave age for unsteady waves is three times greater than that for steady waves; (iv) the vertical component of perturbation velocity is not singular at the critical point in agreement with earlier finding of SHD. In our final remark, we emphasize that since the theoretical and computational results obtained here exceptionally agree with experimental data reported by Snyder gives a great degree of confidence to the theory of air-sea interactions for non-ideal oceanic waves. Also, experiments performed confirm that as bichromatic waves become steeper they form group of waves.

Acknowledgment

This work is supported by DoD-HPCMO under the contract number N62306-99-D-B004.

References

[1] S. E. Belcher and J. C. R. Hunt, Turbulent shear flow over slowly moving waves, J. Fluid Mech. 251 (1993), 109.

[2] S. E. Belcher and J. C. R. Hunt, Turbulent flow over hills and waves, Ann. Rev. Fluid Mech. 30 (1998), 507.

[3] S. E. Belcher, J. C. R. Hunt and J. E. Cohen, Turbulent flow over growing waves, Proceedings of IMA Conference on Wind over Waves, S. G. Sajjadi, N. H. Thomas and J. C. R. Hunt, eds., Oxford University Press, 1999, pp. 19-30.

[4] G. Burgers and V. K. Makin, Boundary-layer model results for wind-sea growth, J. Physical Oceanography 213 (1993), 372.

[5] D. Chalikov, The parameterization of the wave boundary layer, J. Physical Oceanography 25 (1995), 1333.

[6] H. Charnock, Wind stress on a water surface, Q. J. R. Met. Soc. 81 (1955), 639.

[7] J. E. Cohen and S. E. Belcher, Turbulent shear flow over fast-moving waves, J. Fluid Mech. 386 (1999), 345.

[8] S. Conte and J. W. Miles, On the numerical integration of the Orr-Sommerfeld equation, J. Soc. Indust. Appl. Math. 7 (1959), 361.

[9] A. J. Croft and S. G. Sajjadi, A mechanism for the transferring energy from wind to Stokes wave, Math. Eng. Ind. 4 (1993), 23.

[10] F. W. Dobson, Measurements of atmospheric pressure on wind-generated sea waves, J. Fluid Mech. 48 (1971), 91.

[11] M. A. Donelan, F. W. Dobson, S. D. Smith and R. J. Anderson, On the dependence of sea surface roughness on wave development, J. Physical Oceanography 23 (1993), 2143.

[12] K. Hasselmann, Ocean circulation and climate change, Tellus A 43 (1991), 4.

[13] G. Ierley and J. W. Miles, On Townsends rapid-distortion model of the turbulent-wind-wave problem, J. Fluid Mech. 435 (2001), 175.

[14] S. J. Jacobs, An asymptotic theory for the turbulent flow over a progressive wave, J. Fluid Mech. 174 (1987), 69.

[15] P. A. E. M. Janssen, Quasilinear approximation for the spectrum of wind generated ocean waves, J. Fluid Mech. 48 (1982), 91.

[16] P. A. E. M. Janssen, Wave-induced stress and the drag of air flow over sea waves, J. Physical Oceanography 19 (1989), 745.

[17] P. A. E. M. Janssen, Quasi-linear theory of wind wave generation applied to wave forecasting, J. Physical Oceanography 21 (1991), 1631.

[18] P. A. E. M. Janssen, K. Hasselmann, S. Hasselmann and G. J. Komen, Parameterization of source terms and the energy balance in a growing wind sea, Dynamics and Modelling of Ocean Waves, Cambridge University Press, 1994.

[19] P. A. E. M. Janssen, The Interaction of Ocean Waves and Wind, Cambridge University Press, 2004.

[20] H. Jeffreys, On the formation of water waves by wind, Proc. R. Soc. Lond. A 107 (1925), 189.

[21] G. J. Komen, L. Cavaleri, M. A. Donelan, K. Hasselmann, S. Hasselmann and P. A. E. M. Janssen, Dynamics and Modelling of Ocean Waves, Cambridge University Press, 1994.

[22] H. Lamb, Hydrodynamics, 6th ed., Cambridge University Press, 1932.

[23] M. J. Lighthill, Physical interpretation of the mathematical theory of wave generation by wind, J. Fluid Mech. 14(3) (1962), 385.

[24] C. C. Lin, The Theory of Hydrodynamic Stability, Cambridge University Press, 1955.

[25] M. S. Longuet-Higgins, Action of a variable stress at the surface of water waves, Phys. Fluids. 12 (1969), 737.

[26] N. Maat, C. Kraan and W. A. Oost, The roughness of wind waves, Boundary-Layer Meteorology 54 (1991), 89.

[27] V. K. Makin, V. N. Kudryavtsev and C. Mastenbroek, Drag of the sea surface, Boundary-Layer Meteorology 73 (1995), 159.

[28] C. Mastenbroek, V. K. Makin, M. H. Garat and J. P. Giovanangeli, Experimental evidence of the rapid distortion of turbulence in air flow over waves, J. Fluid Mech. 318 (1996), 273.

[29] J. W. Miles, On the generation of surface waves by shear flows, J. Fluid Mech. 3 (1957), 185.

[30] J. W. Miles, On the generation of surface waves by shear flows. Part 2, J. Fluid Mech. 6 (1959), 568.

[31] J. W. Miles, On the generation of surface waves by shear flows. Part 5, J. Fluid Mech. 30 (1967), 163.

[32] J. W. Miles, Surface-wave generation revisited, J. Fluid Mech. 256 (1993), 427.

[33] J. W. Miles, Surface-wave generation: a viscoelastic model, J. Fluid Mech. 322 (1996), 131.

[34] L. M. Milne-Thomson, Theoretical Hydrodynamics, 5th ed., Macmillan, 1968.

[35] T. E. Nordeng, On the wave age dependent drag coefficient roughness length at sea, J. Geophysical Research 96 (1991), 7167.

[36] O. M. Phillips, On the generation of waves by a turbulent wind, J. Fluid Mech. 2 (1957), 417.

[37] O. M. Phillips, Dynamics of the Upper Ocean, 2nd ed., Cambridge University Press, 1977.

[38] W. J. Plant, A relationship between wind shear stress and wave slope, J. Geophysical Research 87, C3 (1984), 1961-1967.

[39] S. G. Sajjadi, Shearing flow over Stokes waves, Technical Report, Coventry Polytechnic, 1988.

[40] S. G. Sajjadi, J. Wakefield and A. J. Croft, On the growth of a fully nonlinear Stokes wave by turbulent shear flow. Part 1. Eddy-viscosity model, Math. Eng. Ind. 6 (1997), 185.

[41] S. G. Sajjadi, On the growth of a fully nonlinear Stokes wave by turbulent shear flow. Part 2. Rapid distortion theory, Math. Eng. Ind. 6 (1998), 247.

[42] S. G. Sajjadi, N. H. Thomas and J. C. R. Hunt, Wind-Over-Wave Couplings: Perspectives and Prospects, Oxford University Press, 1999.

[43] S. G. Sajjadi, Interaction of turbulence due to tropical cyclones with surface waves, Adv. Appl. Fluid Mech. 1(2) (2007), 101.

[44] S. G. Sajjadi, J. C. R. Hunt and F. Drullion, Asymptotic multi-layer analysis of wind over unsteady monochromatic surface waves, J. Eng. Math 84(1) (2014), 73. [Referred to SHD in the manuscript.]

[45] S. G. Sajjadi, On the generation of weakly nonlinear surface waves by shear flows, Adv. Appl. Fluid Mech. 18(2) (2015), 305.

[46] S. G. Sajjadi, An asymptotic analysis for generation of unsteady surface waves on deep water by turbulence, Adv. Appl. Fluid Mech. 19(1) (2016), 101.

[47] S. G. Sajjadi and F. Drullion, A numerical study of turbulent flow over growing monochromatic and Stokes waves, Adv. Appl. Fluid Mech. 19(1) (2016), 47.

[48] R. L. Snyder, F. W. Down, J. A. Elliot and R. B. Long, Array measurements of atmospheric pressure fluctuations above gravity waves, J. Fluid Mech. 102 (1981), 1.

[49] W. Stewart, Mechanics of the air sea interface, Phys. Fluids Suppl. 10 (1969), 547.

[50] P. P. Sullivan, J. C. McWilliams and C. H. Moeng, Simulation of turbulent flow over idealized water waves, J. Fluid Mech. 404 (2000), 47.

[51] H. L. Tolman and D. Chalikov, Source terms in a third-generation wind wave model, J. Physical Oceanography 26 (1996), 2497.

[52] H. L. Tolman, Alleviating the garden sprinkler effect in wind wave models, Ocean Modeling 4 (2002a), 269.

[53] H. L. Tolman, The 2002 release of WAVEWATCH III, 7th International Workshop on Wave Hindcasting and Forecasting, 2002b, pp. 188-197.

[54] J. Touboul, C. Kharif, E. Pelinovsky and J. P. Giovanangeli, On the interaction of wind and steep gravity wave groups using Miles' and Jeffreys' mechanisms, Nonlin. Processes Geophys. 15 (2008), 1023.

[55] A. A. Townsend, Flow in a deep turbulent boundary layer over a surface distorted by water waves, J. Fluid Mech. 55 (1972), 719.

[56] A. A. Townsend, The Structure of Turbulent Shear Flow, 2nd ed., Cambridge University Press, 1976.

[57] A. A. Townsend, Sheared turbulence and additional distortion, J. Fluid Mech. 98 (1980), 171.

[58] Y. S. Tsai, A. J. Grass and R. R. Simons, On the spatial linear growth of gravity-capillary water waves sheared by laminar air flow, Phys. Fluids 17(9) (2005), 095101.

[59] F. Ursell, Wave generation by wind, Surveys in Mechanics, G. K. Batchelor and R. M. Davies, eds., Cambridge University Press, 1956.

[60] C. A. van Duin and P. A. E. M. Janssen, An analytical model of the generation of surface gravity waves by turbulent air flow, J. Fluid Mech. 236 (1992), 197.

Appendix A. Numerical Solution

The energy transfer parameters α_j and β_j are evaluated by numerical integration of the Orr-Sommerfeld equation, derived in Section 4[†]

$$(f^2\Theta')' - f^2\Theta = (iR)^{-1}(f\Theta')'''. \tag{A1}$$

Following the notations in Section 4, letting $\Theta = -ik\phi f'$ and following Croft and Sajjadi [9], we may express the solution of (A1) as a combination of inviscid plus viscous solutions $\phi + h \equiv F$, where $\phi(\eta)$ satisfies the following boundary value problem:

$$f\left(\frac{d^2\phi}{d\xi^2} - \phi\right) - \left(\frac{d^2 f}{d\xi^2}\right)\phi = 0 \qquad (0 < \xi_0 \le \xi < \infty) \tag{A2}$$

subject to the boundary conditions

$$\phi_0 = f_0 \qquad (\xi = \xi_0), \tag{A2a}$$

$$\frac{d\phi}{d\xi} + \phi \to 0 \qquad (\xi \to \infty). \tag{A2b}$$

As was shown by Croft and Sajjadi [9], the asymptotic analysis for large R indicates that the viscous solution approximately obeys the equation

[†]For clarity sake, we will describe the procedure for the fundamental harmonic $j = 1$.

$$\frac{d^4h}{d\xi^4} - i\gamma(\xi)\frac{d^2h}{d\xi^2} = 0 \tag{A3}$$

subject to the boundary conditions

$$h_0 = 0, \quad h_0'' = 1, \tag{A4}$$

$$h' = h''' = 0 \text{ as } \xi \to \infty, \tag{A5}$$

where

$$f(\xi) = \log(\xi/\xi_c) \qquad (\xi_c > \xi_0) \tag{A6}$$

and

$$\gamma(\xi) = Rf(\xi). \tag{A7}$$

To integrate equation (A3) we first reduce it to a pair of second order differential equations

$$\left.\begin{aligned} h'' &= \chi, && \text{subject to } h_0 = 0 \text{ and } h' \to 0 \text{ as } \xi \to \infty \\ \chi'' - i\gamma\chi &= 0, && \text{subject to } \chi_0 = 1 \text{ and } \chi' \to 0 \text{ as } \xi \to \infty \end{aligned}\right\}. \tag{A8}$$

The integration of equations (A8) poses no real difficulty, however the solution of equation (A2) poses a major difficulty due to the singular behaviour of the equation around $\xi = \xi_c$.

Note that ξ is confined to the real axis except in the neighbourhood of the regular singular point $\xi = \xi_c$, where the path of integration must be taken under the singularity. The components of this singularity are 0 and 1, and there exists only one analytic solution, $\phi_1 = O(f)$, in this neighbourhood. The second linearly independent solution has a logarithmic branch point there and may be posed as

$$\phi_2 = \phi_1 \log f + \phi_3, \tag{A9}$$

where ϕ_3 is analytic and $O(1)$ in the neighbourhood of $f = 0$ and ϕ_1 is the regular solution of (A2).

Substituting (A9) into (A2) we obtain the following inhomogeneous equation:

$$f\left(\frac{d^2\phi_3}{d\xi^2}-\phi_3\right)-\left(\frac{d^2 f}{d\xi^2}\right)\phi_3=-f\log f\,\frac{d^2\phi_1}{d\xi^2}-2\frac{df}{d\xi}\frac{d\phi_1}{d\xi}$$

$$-\left[\frac{d^2 f}{d\xi^2}-\frac{1}{f}\left(\frac{df}{d\xi}\right)^2-\left(f-\frac{d^2 f}{d\xi^2}\right)\log f\right]\phi_1, \qquad \text{(A10)}$$

where ϕ_1 is the regular solution of (A2), namely

$$f\left(\frac{d^2\phi_1}{d\xi^2}-\phi_1\right)-\left(\frac{d^2 f}{d\xi^2}\right)\phi_1=0. \qquad \text{(A11)}$$

The procedure adopted here is to determine ϕ_1 and ϕ_3 successively and then to combine ϕ_1 and ϕ_2 to satisfy (A2a, b).

Substituting (A9) into (A2a, b), we obtain the following boundary conditions:

$$\left.\begin{array}{ll}\phi_1=G & \text{and } \phi_2=G(1-\log f) \text{ at } \xi=\xi_0\\ \dfrac{d\phi_1}{d\xi}+\phi_1=0 & \text{and } \dfrac{d\phi_2}{d\xi}=\phi_2=-H \text{ as } \xi\to\infty\end{array}\right\}, \qquad \text{(A12)}$$

where

$$G=\phi_1\log f+\phi_2 \text{ evaluated at } \xi=\xi_0,$$

$$H=\phi_1\left(\frac{1}{f}\frac{df}{d\xi}+\log f\right)+\left(\frac{d\phi_1}{d\xi}\log f\right) \text{ as } \xi\to\infty.$$

We discretize the above system of equation using central differences and seek their solutions over an unsteady Stokes wave defined by (4.2) and then calculate the resulting pressure acting on the surface, from (4.15c), where the energy transfer parameters α and β are calculated according to

$$\alpha+i\beta=f_0\left(\frac{dF}{d\xi}-\frac{df}{d\xi}\right)_0. \qquad \text{(A13)}$$

Note that, the energy transfer to the Stokes wave at the surface is proportional to β, namely

$$\beta = -\pi |F|_c^2 (f_c''/f_c'), \tag{A14}$$

where the subscript c implies evaluation at the singular point $\xi = \xi_c$,

$$\xi_c = \Omega f_0^{-2} e^{-f_0}, \quad \frac{c}{U_1} = -f_0 = \log(\xi_c/\xi_0), \quad \Omega = g\xi_0/U_1^2 \tag{A15}$$

and $\Omega = O(10^{-3} - 10^{-2})$ is Charnock's [6] constant.

The solution of the boundary value problem (A2) posed here is solved in the following manner. We first solve (A2) for the regular solution ϕ_1, then we substitute (A9) in (A2) and solve the resulting equation for ϕ_3. Having done this we combine ϕ_1 and ϕ_2 to satisfy the boundary conditions (A2a, b), and finally determine β through either (A13) or (A14).

In carrying out this program numerically for the solution of equation (A2) the velocity f provides a more convenient scale than the independent variable ξ. Under the change of independent variable (A6), the boundary value problem (A2), (A2a, b) becomes

$$L\phi = f\left(\frac{d^2\phi}{df^2} - \frac{d\phi}{df}\right) + (1 - \xi_c^2 f e^{2f})\phi = 0 \quad (-\infty < f_0 \le f \le \infty), \tag{A16}$$

$$\phi_0 = f_0, \tag{A16a}$$

$$\frac{d\phi}{df} + \xi_c e^f \phi \to 0 \quad (f \to \infty), \tag{A16b}$$

where (A16) defines the operator L, and the singularity now appears at $f = 0$.

Applying the method of Frobenius we can now obtain series expansions valid about the singularity $f = 0$ for two linearly independent solutions. If we let

$$\phi = \sum_{k=1}^{\infty} b_k f^{k+r}, \quad b_0 \neq 0$$

and expand the exponential in (A16) in powers of f, we obtain

$$\sum_{k=1}^{\infty} b_k (k+r)(k+r-1) f^{k+r-1} - \sum_{k=1}^{\infty} b_k (k+r) f^{k+r}$$

$$+ [1 - \xi_c^2 f(1 + 2f + 2f^2 + \cdots)] \sum_{k=1}^{\infty} b_k f^{k+r} = 0.$$

Equating coefficients of f^{r-1} we find that $r = 0$ or $r = 1$. Now equating coefficients of f^r, f^{r+1}, f^{r+2}, ... for $r = 1$, we obtain b_k's for $k \geq 1$ in terms of b_0. Without loss of generality we set $b_0 = 1$, thus the series for the regular solution ϕ_1 is

$$\phi_1 = f + \frac{1}{6}\xi_c^2 f^3 + \frac{7}{36}\xi_c^2 f^4 + \frac{\xi_c^2}{240}(31 + 2\xi_c^2) f^5$$

$$+ \frac{\xi_c^2}{5400}(333 + 101\xi_c^2) f^6 + \cdots. \tag{A17}$$

To obtain the logarithmic solution we substitute (A9) into (A16) and, observing that $L\phi_1 = 0$, we obtain

$$L\phi_3 = (1 + f^{-1})\phi_1 - 2\frac{d\phi_1}{df} \tag{A18}$$

as the inhomogeneous differential equation for ϕ_3. Substituting (A17) into (A18) and again expanding, we obtain

$$\phi_3 = -1 + \frac{1}{2}(1 + \xi_c^2) f^2 + \frac{5}{180}(3 + 20\xi_c^2) f^3$$

$$+ \frac{1}{432}(6 - 137\xi_c^2 - 18\xi_c^4) f^4$$

$$+\frac{79}{900}\left(\frac{45}{1896}+\frac{179}{632}\xi_c^2-\xi_c^4\right)f^5+\cdots. \tag{A19}$$

The general solution of (A16) is

$$\phi = A\phi_1 + B\phi_2, \tag{A20}$$

where A and B are constants to be chosen so as to satisfy the boundary conditions (A16a, b). The equations for determining A and B are:

$$\left.\begin{aligned} &A\phi_1(f_0) + B\phi_2(f_0) = f_0, \\ &A\left[\frac{d\phi_1}{df}+\xi_c e^f\phi_1\right]_{f_+} + B\left[\frac{d\phi_2}{df}+\xi_c e^f\phi_2\right]_{f_+} = 0 \end{aligned}\right\}, \tag{A21}$$

where f_+ is, for the purpose of numerical integration, infinite; the actual value of f_+ varies, depending upon the parameters ξ_c and Ω.

The numerical integration for boundary value problems, defined by (A8), was performed using a five point central difference approximation. Writing any of these equations in the form

$$\Phi'' - u\Phi = w,$$

where $\Phi \equiv \{\phi_1, \phi_3, h, \chi\}$, and discretizing them using following approximations:

$$\Phi = \frac{1}{360}(\Phi_{i+2} + 56\Phi_{i+1} + 246\Phi_i + 56\Phi_{i-1} + \Phi_{i-2}),$$

$$\Phi'' = \ell^{-2}\left(\Delta_i^2 + \frac{1}{12}\Delta_i^4\right)\Phi$$

here Δ_i is the central difference operator and ℓ is the uniform step length, we obtain quindiagonal matrix equations

$$\mathscr{A}\boldsymbol{\Phi} = \boldsymbol{w}.$$

These equations are then solved using the standard Gauss elimination technique.

The presence of the singularity at $f = 0$ necessitated the evaluation of the series (A17) and (A19) at some point f_1 sufficiently removed from the singularity before the numerical solution could be carried out. From these series we obtained ϕ_1 and ϕ_3 and their derivatives at f_1. The value of f_1 chosen varied from 10^{-4} to 10^{-7} depending upon the value of ξ_c. The lower limit of integration was fixed at f_0. The numerical integration for the viscous equation (A3) was then performed using the central finite difference approximation of the coupled system (A8) and the result was combined with the numerical solution of (A2) to yield the solution to the Orr-Sommerfeld equation (A1). Having obtained the numerical solution to (A2), β was calculated using equation (A14).